FACULTY
OF MATHEMATICS
AND PHYSICS
Charles University

MASTER THESIS

Bc. Radka Kváčová

Numerical solution of porous media flow with a dual-permeability model

Department of Numerical Mathematics

I declare that I carried out this master thesis independently, and only with the cited sources, literature and other professional sources. It has not been used to obtain another or the same degree.

I understand that my work relates to the rights and obligations under the Act No. 121/2000 Sb., the Copyright Act, as amended, in particular the fact that the Charles University has the right to conclude a license agreement on the use of this work as a school work pursuant to Section 60 subsection 1 of the Copyright Act.

In . . . . date . . . .
                                                                              Author's signature

Title: Numerical solution of porous media flow with a dual-permeability model

Author: Bc. Radka Kváčová

Department: Department of Numerical Mathematics

Supervisor: prof. RNDr. Vít Dolejší, Ph.D., DSc., Department of Numerical Mathematics

Abstract: The flow in porous media can be described by the Richards equation. However, porous media often exhibit a variety of heterogeneities, thus treating a porous medium as homogeneous does not often fit the reality well. Therefore, we describe the flow in the porous medium using the Richards equation with the dual-permeability model, which assumes that the porous medium can be separated into two different media. This thesis is concerned with the numerical solution of the Richards equation with the dual-permeability model. We present the derivation of the dual-permeability model, and for the numerical solution, we use the space-time discontinuous Galerkin method. This produces a system of nonlinear algebraic equations that need to be linearized. We perform a 1D experiment to verify the method and, finally, we present a 2D single-ring experiment to demonstrate the method.

Keywords: Porous media flow, Richards equation, dual permeability, numerical solution.

Contents

List of physical quantities

Used physical quantities and their units using the international system of units:

- [kg] ... mass,

- [m] ... length,

- [s] ... time,

- [−] ... dimensionless.

However, physical quantities concerning porous media are often expressed in [cm/day] units, which we will be using later.

Introduction

Mathematical modeling of flow in porous media is an important field in hydrogeology, mining industry or simulations of diffusion of toxic substances for environmental protection. One can imagine a water soaking through a dam, which is composed of different materials, such as clay or gravel. Although porous media often show a variety of heterogeneiteis such as cracks or fissures, we will consider a porous medium as a continuum with given physical properties. This process can be described by the Richards equation (see Chapter 1)

$$\frac{\partial \vartheta(\Psi - z)}{\partial t} - \nabla \cdot (\mathbf{K}(\Psi - z)\nabla\Psi) + \frac{S}{\rho_{water}} = 0,$$

where the unknown scalar function Ψ is called the hydraulic head. Moreover, function $\mathbf{K}$ is the hydraulic conductivity, ϑ is the active porous volume, z is the geodetic head and S is the sink term.

However, treating porous media as homogeneous does not often correspond to the reality, especially if the porous medium contains different materials. Thus, we will assume that porous medium can be described by two different porous media, see Figure 1.
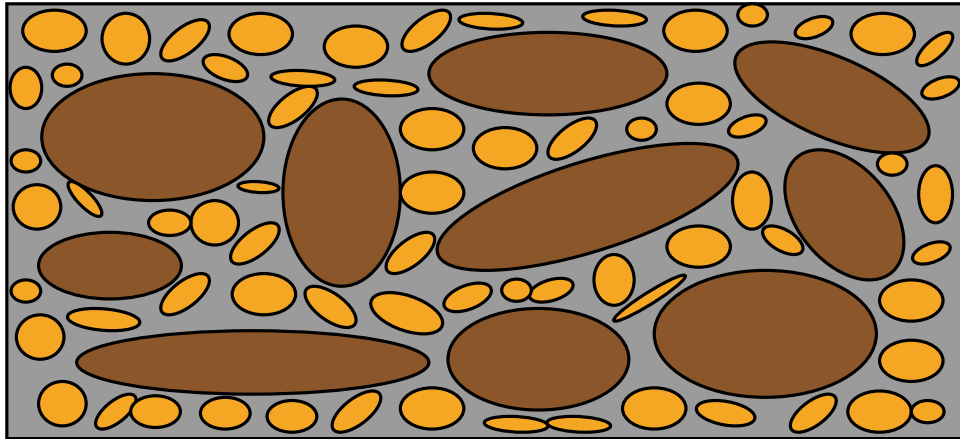
Figure 1: Example of a porous medium at the microscopic level.

In this work, we deal with such a flow in porous media that can be described by the dual permeability model [1]. It means the porous medium can be separated into two distinct pore systems, one associated with a macropore network (fracture pore system $_f$) and the other with a less permeable pore system such as rock matrix blocks (matrix pore system $_m$). As the description above indicates, this problem can be described by a pair of coupled equations

$$\begin{aligned}
\frac{\partial \vartheta_f(\Psi_f - z)}{\partial t} - \nabla \cdot (\mathbf{K}_f(\Psi_f - z)\nabla\Psi_f) &= -S_f - \frac{\Gamma_w}{w_f}, \\
\frac{\partial \vartheta_m(\Psi_m - z)}{\partial t} - \nabla \cdot (\mathbf{K}_m(\Psi_m - z)\nabla\Psi_m) &= -S_m + \frac{\Gamma_w}{1 - w_f}.
\end{aligned} \tag{1}$$

The solution of (1) is a pair of functions $(\Psi_f, \Psi_m) = (\Psi_f(\mathbf{x}, t), \Psi_m(\mathbf{x}, t))$ representing the hydraulic head Ψ_f of the fracture pore system and the hydraulic

head Ψ_m of the matrix pore system. The other functions in (1) will be described later.

Richards equation (1) is a degenerate parabolic equation, because the function ϑ and the matrix $\mathbf{K}$ are nonlinear and can degenerate, i.e., for some porous media it holds

$$\lim_{\psi \to -\infty} \vartheta(\psi) = 0, \quad \lim_{\psi \to 0} \vartheta'(\psi) = \infty, \quad \lim_{\psi \to -\infty} ||\mathbf{K}(\psi)|| = 0,$$

where $\psi = \Psi - z$.

Following [2], we discretize problem (1) by the space-time discontinuous Galerkin method, which provides high accuracy with respect to space and time and is suitable for the mesh adaptation. We present the governing equation and derive the Richards equation with the dual-permeability model. We also formulate the dual-permeability model in a weak sense and subsequently we present the discretization with respect to the space and to the time. This leads to the system of nonlinear algebraic equations for each time level, therefore a linearization process is required. To complete our solution strategy, we will briefly mention stopping criteria for solving the linearized systems and mesh adaptation. All the computations are performed using the ADGFEM [3] framework. Finally, several numerical experiments are presented. First, we verify the method on a thin rectangular domain. Afterwards, we perform a single ring experiment, which is commonly used for estimating hydraulic properties of soil. This experiment will be also performed with the mesh adaptation.

1. Governing equation

In this chapter, we derive the dual-permeability Richards equation. We will assume that the domain Ω is a porous medium with flowing water, consisting of soil aggregates or rocks and of fracture pore network. Sections 1.1 - 1.4 will cover the derivation of the Richards equation, and in Section 1.5 we introduce the dual-permeability model.

1.1 Mass conservation law

We phenomenologically postulate the law of conservation of mass. Let $t \in (0, T)$ and $\Omega \subset \mathbb{R}^2$ be an open domain. Consider a volume $V \subset \Omega$ arbitrary but fixed in time t. We define a mass of fluid in volume V as q and its density as ρ. Further, we define a volumetrix flux $\mathbf{q}$, which is a vector field describing the way the quantity q flows and represents the rate of volume flow through a unit area.

The total mass q of a fluid in V is defined by the integral

$$q = q(t) = \int_V \rho(\mathbf{x}, t) \, \mathrm{d}V,$$

and it can change in time if fluid flows through the surface (inside or outside). This rate that q is flowing can be expressed by the volumetrix flux in integral form

$$\int_{\partial V} \rho_{fluid} \, \mathbf{q}(\mathbf{x}, t) \cdot \mathbf{n}(\mathbf{x}, t) \, \mathrm{d}S,$$

where $\mathbf{n}$ is outward unit normal.

Because of properties of porous medium, we will also consider a sink term S representing the sink (typically plant root water extraction) of q as it is also contributing to the total quantity of fluid in V. We can express the total mass contributed by the sink term S as

$$\int_V S(\mathbf{x}, t) \, \mathrm{d}V.$$

Finally, the integral form of the law of conservation of mass reads

$$\frac{\partial}{\partial t} \int_V \rho(\mathbf{x}, t) \, \mathrm{d}V + \int_{\partial V} \rho_{fluid} \, \mathbf{q} \cdot \mathbf{n} \, \mathrm{d}S + \int_V S \, \mathrm{d}V = 0.$$

Suppose $\mathbf{q}$ is continuously differentiable on a neighborhood of V. Then using the divergence theorem and the fact that V is independent of t we get

$$\int_V \frac{\partial \rho}{\partial t} + \nabla \cdot (\rho_{fluid} \, \mathbf{q}) + S \, \mathrm{d}V = 0 \quad \forall V \subset \Omega$$

resulting in continuity equation

$$\frac{\partial \rho}{\partial t} + \nabla \cdot (\rho_{fluid} \, \mathbf{q}) + S = 0 \quad \text{in } \Omega \times (0, T). \tag{1.1}$$

1.2 Volumetric water content

We will consider a volumetric water content θ. At the point $\mathbf{x} \in \Omega$ and in time $t \in (0, T)$ the function $\theta(\mathbf{x}, t)$ represents a relative volume of fluid in an infinitesimally small porous domain. Hence θ is defined as

$$\theta = \frac{V_{fluid}}{V_{total}},$$

where V_{fluid} is the infinitesimal volume of water and $V_{total} = V_{fluid} + V_{air} + V_{soil}$ is the sum of infinitesimal volumes of fluid, air and soil. Thus, we can express rhe density ρ as

$$\rho(\mathbf{x}, t) = \rho_{water}\, \theta(\mathbf{x}, t).$$

Considering a compressible porous medium, then the relative volume of fluid contributes to the following relation:

$$\vartheta(\mathbf{x}, t) := \theta(\mathbf{x}, t) + \frac{S_s}{\theta_s} \int_{-\infty}^{\psi} \theta(s)\, \mathrm{d}s, \tag{1.2}$$

where we define the active porous volume $\vartheta(\psi)$ and $S_s > 0$ is the storativity. Then for the compressible medium, we correct the density ρ as

$$\rho(\mathbf{x}, t) = \rho_{water}\, \vartheta(\mathbf{x}, t). \tag{1.3}$$

We can deduce that volumetric water content θ depends on the pressure head ψ as $\psi(\mathbf{x}, t)$ corresponds to the height of a liquid column at point $\mathbf{x}$. Thus, we can write $\theta = \theta(\psi)$. This relation is represented by the water retention curve, which is a continuous function satisfying

$$\lim_{\psi \to -\infty} \theta(\psi) = \theta_r \quad \text{and} \quad \theta(\psi) = \theta_s \quad \text{for } \psi \geq 0,$$

where θ_r is the residual water content (limiting water content for inducing unsaturated flow) and θ_s is the saturated water content (state of maximal water saturation).

Further, we will use the proposed van Genuchten model [4] for the water retention curve $\theta(\psi)$:

$$\theta(\psi) = \begin{cases} \theta_r + \frac{\theta_s - \theta_r}{(1 + (-\alpha\psi)^n)^m} & \text{for } \psi \leq 0, \\ \theta_s & \text{for } \psi \geq 0, \end{cases} \tag{1.4}$$

where m and n are the measure of the pore-size distribution and α is related to the inverse of the air entry suction.

1.3 Darcy-Buckingham's law

Darcy-Buckingham's law describes the macroscopic flow of a fluid through an unsaturated porous medium and it represents the relations between the volumetric flux $\mathbf{q}$ and the hydraulic head Ψ. It states [5]

$$\mathbf{q} = -\mathbf{K}(\theta)\, \nabla\Psi,$$

where $\mathbf{K}(\theta)$ is the unsaturated hydraulic conductivity.

The hydraulic head Ψ consists of the pressure head ψ and the geodetic head z. The geodetic head at a point $\mathbf{x} = (x, z)$ has the value z. Then

$$\Psi(\mathbf{x}, t) = \psi(\mathbf{x}, t) + z.$$

The hydraulic conductivity $\mathbf{K}$ is defined as

$$\mathbf{K}(\psi) = K_r(\psi)\mathbf{K}_s,$$

where $\mathbf{K}_s$ is the saturated hydraulic conductivity and K_r is the relative hydraulic conductivity, which is a reduction of the saturated hydraulic conductivity, so $K_r \in (0, 1]$. If the porous medium is isotropic, we can write $\mathbf{K}_s$ as

$$\mathbf{K}_s = K_s \mathbf{I},$$

where $\mathbf{I}$ is the identity matrix.

Since there is a relation for $\theta(\psi)$, we can also consider a relation for the function $K_r(\psi)$. This constitutive relation is expressed by the Mualem function [6]. Combined with the van Genuchten function for the retention curve (1.4) the formula reads

$$K_r(\psi) = \begin{cases} \frac{(1 - (-\alpha\psi)^{nm}(1 + (-\alpha\psi)^n)^{-m})^2}{(1 + (-\alpha\psi)^n)^{m/2}} & \text{for } \psi \leq 0, \\ 1 & \text{for } \psi \geq 0, \end{cases} \tag{1.5}$$

where parameters α, m and n were already explained in (1.4).

Thus, in terms of Ψ, Darcy-Buckingham's law reads

$$\mathbf{q} = -\mathbf{K}(\Psi - z)\nabla\Psi. \tag{1.6}$$

1.4 Richards equation

Moreover, we introduce the derivative of the water retention curve, which is called the water retention capacity $C(\psi)$ and it is defined as

$$C(\psi) := \frac{\mathrm{d}\theta(\psi)}{\mathrm{d}\psi} = \begin{cases} \frac{(\theta_s - \theta_r)mn\alpha(-\alpha\psi)^{n-1}}{(1 + (-\alpha\psi)^n)^{m+1}} & \text{for } \psi \leq 0, \\ 0 & \text{for } \psi \geq 0. \end{cases}$$

Remark 1. Note, that the integral

$$\int_{-\infty}^{\psi} \theta(s)\,\mathrm{d}s$$

in (1.2) is infinite in general. It is mathematically correct to write the integral as

$$\int_{-c}^{\psi} \theta(s)\,\mathrm{d}s,$$

where c is sufficiently large, but it is common to write it as $c = \infty$, because Richards equation uses only the derivative of this term. We can write

$$\frac{\mathrm{d}}{\mathrm{d}\psi}\int_{-\infty}^{\psi} \theta(s)\,\mathrm{d}s = \frac{\mathrm{d}}{\mathrm{d}\psi}\int_{-\infty}^{\psi^*} \theta(s)\,\mathrm{d}s + \frac{\mathrm{d}}{\mathrm{d}\psi}\int_{\psi*}^{\psi} \theta(s)\,\mathrm{d}s$$

$$= 0 + \theta(\psi)$$

Thus, we can write the derivative of the active porous volume ϑ

$$\frac{\mathrm{d}\vartheta}{\mathrm{d}\psi} = C(\psi) + \frac{S_s}{\theta_s}\theta(\psi).$$

In terms of Ψ, we denote

$$\gamma(\Psi - z) := C(\Psi - z) + \frac{S_s}{\theta_s}\theta(\Psi - z), \qquad (1.7)$$

and because $\frac{\partial \Psi}{\partial t} = \frac{\partial \psi}{\partial t}$, we can write

$$\frac{\partial \vartheta}{\partial t} = \frac{\mathrm{d}\vartheta}{\mathrm{d}\psi}\frac{\partial \psi}{\partial t} = \gamma(\Psi - z)\frac{\partial \Psi}{\partial t}. \qquad (1.8)$$

Returning to the derived continuity equation (1.1), substituting (1.3), (1.6) and using (1.8) yields Richards equation

$$\gamma(\Psi - z)\frac{\partial \Psi}{\partial t} - \nabla \cdot (\mathbf{K}(\Psi - z)\nabla\Psi) + \frac{S}{\rho_{water}} = 0, \qquad (1.9)$$

where Ψ is the unknown function, the function γ and the matrix $\mathbf{K}$ are known from the relations (1.7), (1.5) and S is the sink term.

1.5 Dual-permeability model

We follow continuous mixture theory, namely the assumption of the equipresence of all components. In our dual-permeability approach, at each point, we will assume that the medium can be separated into two distinct pore systems (fracture and matrix domain), both of which are treated as homogeneous media with separated hydraulic and solute transport properties. The dual-permeability medium is considered to be a superposition of these two systems over the same volume [1].

Moreover, we assume that these two separate porous media can be described by the equations derived above. Hence, we denote equation (1.9) with the subscript f for the fracture medium and with the subscript m for the matrix medium. However, these equations do not form the coupled system covering our medium, since they are independent, even though there is also some exchange of the physical quantities between them.

Hence, we denote Γ_w as the term representing the exchange between the fracture and the matrix pore system, which is weighted by the volume fraction of the corresponding components. We consider w_f as the fracture weight, i.e., the volume of the fracture pore system relative to the total pore system, defined as

$$w_f = \frac{\text{volume of fracture medium}}{\text{volume of whole medium}}.$$

Further, we assume that the volume additivity constraint (quasi-incompressibility) holds, i.e., $w_m + w_f = 1$, where w_m is the matrix weight, as the components of porous media are solid and their volumes do not penetrate each other on the microscale level.

Using the mentioned first-order coupling term, we can write the fully coupled dual-permeability model as

$$\gamma_f(\Psi_f - z)\frac{\partial \Psi_f}{\partial t} - \nabla \cdot (\mathbf{K}_f(\Psi_f - z)\nabla \Psi_f) = -\frac{S_f}{\rho_{water}} - \frac{\Gamma_w}{w_f},$$
$$\gamma_m(\Psi_m - z)\frac{\partial \Psi_m}{\partial t} - \nabla \cdot (\mathbf{K}_m(\Psi_m - z)\nabla \Psi_m) = -\frac{S_m}{\rho_{water}} + \frac{\Gamma_w}{w_m}. \quad (1.10)$$

For further derivations and computations, we will omit the sink terms S_f and S_m, because they have negligible influence on our computations.

Exchange term Γ_w

The interactions between the fracture and the matrix pore systems are governed by non-linear processes. Trying to capture these microscopic processes while preserving a relatively simple formula was the objective of [7]. The coupling term Γ_w can be modeled by the first-order exchange term. This assumes the water transfer is proportional to the difference between the pressure heads of the two pore systems and is defined as

$$\Gamma_w = \alpha_w(\psi_f - \psi_m) = \alpha_w(\Psi_m - \Psi_f)$$

for any depth z, where α_w is the first-order transfer coefficient for the water.

The exchange term Γ_w is space and time dependent. If $\Gamma_w > 0$, the water transfer is directed from the fracture system into the matrix system.

We will assume the first-order transfer coefficient for water has the form [7]

$$\alpha_w = \frac{\beta}{a^2}\gamma_w K_a,$$

where K_a is the effective hydraulic conductivity, β is the dimensionless parameter depending on geometry of the aggregates, a represents the distance from the center of a matrix block to the fracture boundary and γ_w is the dimensionless empirical scaling factor.

The representation of the effective hydraulic conductivity was studied in [7]. There were compared several proposals how to set K_a and we will use

$$K_a = \frac{1}{2}\Big(\mathbf{K}_f(\psi_f) + \mathbf{K}_m(\psi_m)\Big).$$

This choice considers both pressure heads for the matrix and for the fracture, thus it can be advantageous during simulation of the water transfer in both directions.

Finally, we can clearly see these two equations are linked, so we can write (1.10) as

$$\gamma_f(\Psi_f - z)\frac{\partial \Psi_f}{\partial t} - \nabla \cdot (\mathbf{K}_f(\Psi_f - z)\nabla \Psi_f) = -\frac{S_f}{\rho_{water}} - \frac{\Gamma_w(\Psi_f, \Psi_m)}{w_f},$$
$$\gamma_m(\Psi_m - z)\frac{\partial \Psi_m}{\partial t} - \nabla \cdot (\mathbf{K}_m(\Psi_m - z)\nabla \Psi_m) = -\frac{S_m}{\rho_{water}} + \frac{\Gamma_w(\Psi_f, \Psi_m)}{w_m}. \quad (1.11)$$

2. Problem formulation

In Section 2.1, we formulate the problem for the closed system of equations. The concept of the weak formulation for the system (1.10) is presented in Section 2.2.

2.1 System of scalar nonlinear parabolic equations

Let $\Omega \subset \mathbb{R}^2$ be a bounded domain with Lipschitz boundary $\partial\Omega = \partial\Omega_D \cup \partial\Omega_N$, $\partial\Omega_D \cap \partial\Omega_N = \emptyset$, corresponding to the Dirichlet and the Neumann boundary part. Let us define time-space cylinder $Q := (0, T) \times \Omega$ and a part of its boundary as $\Sigma := (0, T) \times \partial\Omega$. Moreover, we split the boundary $\Sigma = \Sigma_D \cup \Sigma_N$.

Let us formulate our problem: Find functions

$$\Psi_f : Q \to \mathbb{R},$$
$$\Psi_m : Q \to \mathbb{R},$$

sufficiently smooth, such that following holds:

$$\gamma_f(\Psi_f - z) \frac{\partial \Psi_f}{\partial t} - \nabla \cdot (\mathbf{K}_f(\Psi_f - z)\nabla\Psi_f) = -\frac{\Gamma_w(\Psi_f, \Psi_m)}{w_f} \quad \text{in } Q,$$
$$\gamma_m(\Psi_m - z) \frac{\partial \Psi_m}{\partial t} - \nabla \cdot (\mathbf{K}_m(\Psi_m - z)\nabla\Psi_m) = \frac{\Gamma_w(\Psi_f, \Psi_m)}{1 - w_f} \quad \text{in } Q, \tag{2.1}$$

with the Dirichlet boundary conditions

$$\Psi_f = \Psi_{D_f} \quad \text{on } \Sigma_D,$$
$$\Psi_m = \Psi_{D_m} \quad \text{on } \Sigma_D, \tag{2.2}$$

with the Neumann boundary conditions

$$(\mathbf{K}_f(\Psi_f - z)\nabla\Psi_f) \cdot \mathbf{n} = \Psi_{N_f} \quad \text{on } \Sigma_N,$$
$$(\mathbf{K}_m(\Psi_m - z)\nabla\Psi_m) \cdot \mathbf{n} = \Psi_{N_m} \quad \text{on } \Sigma_N, \tag{2.3}$$

and with the initial conditions

$$\Psi_f(x, t = 0) = \Psi_{f_0} \quad \text{in } \Omega,$$
$$\Psi_m(x, t = 0) = \Psi_{m_0} \quad \text{in } \Omega, \tag{2.4}$$

where $\Psi_{D_f}, \Psi_{D_m}, \Psi_{N_m}, \Psi_{N_f}, \Psi_{m_0}, \Psi_{f_0}$ are given functions and $\mathbf{n}$ is the outer unit normal to Σ_N. We remind that the exchange term Γ_w is dependent on Ψ_f and Ψ_m, i.e., $\Gamma_w = \Gamma_w(\Psi_f, \Psi_m)$.

From now on, we will omit the arguments of $\mathbf{K}_f, \mathbf{K}_m, \gamma_f, \gamma_m$ and Γ_w, if the context is clear.

2.2 Weak formulation

Let us now introduce the weak solution of the above problem. To do this, we need to specify assumptions on the Dirichlet boundary conditions as follows:

$$\Psi_{D_f} = \text{trace of some } \Psi^* \in C([0,T]; H^1(\Omega)) \cap L^\infty(Q) \quad \text{on } \Sigma_D,$$
$$\Psi_{D_m} = \text{trace of some } \Psi^{**} \in C([0,T]; H^1(\Omega)) \cap L^\infty(Q) \quad \text{on } \Sigma_D, \tag{2.5}$$

The Neumann boundary conditions as

$$\Psi_{N_f} \in C([0,T]; L^2(\partial\Omega_N)),$$
$$\Psi_{N_m} \in C([0,T]; L^2(\partial\Omega_N)),$$

and the initial conditions as

$$\Psi_{m_0} \in L^2(\Omega),$$
$$\Psi_{f_0} \in L^2(\Omega).$$

Finally, let us define spaces

$$V_D := \{v \in H^1(\Omega) : v|_{\partial\Omega_D} = 0\}, \quad V := C([0,T]; V_D).$$

Let $\varphi_f, \varphi_m \in V_D$ be arbitrary. We multiply equations (2.1) by φ_f, φ_m, respectively, and integrate over Ω to get

$$\int_\Omega \gamma_f \frac{\partial\Psi_f}{\partial t}\, \varphi_f\, \mathrm{d}\mathbf{x} - \int_\Omega \nabla \cdot (\mathbf{K}_f \nabla\Psi_f)\, \varphi_f\, \mathrm{d}\mathbf{x} = \int_\Omega -\frac{\Gamma_w}{w_f}\, \varphi_f\, \mathrm{d}\mathbf{x},$$

$$\int_\Omega \gamma_m \frac{\partial\Psi_m}{\partial t}\, \varphi_m\, \mathrm{d}\mathbf{x} - \int_\Omega \nabla \cdot (\mathbf{K}_m \nabla\Psi_m)\, \varphi_m\, \mathrm{d}\mathbf{x} = \int_\Omega \frac{\Gamma_w}{w_m}\, \varphi_m\, \mathrm{d}\mathbf{x}.$$

Using the Green's theorem and the conditions (2.3), we obtain

$$\int_\Omega \nabla \cdot (\mathbf{K}_f \nabla\Psi_f)\, \varphi_f\, \mathrm{d}\mathbf{x} = \int_{\Sigma_N} \Psi_{N_f}\, \varphi_f\, \mathrm{d}S - \int_\Omega (\mathbf{K}_f \nabla\Psi_f) \cdot \nabla\varphi_f\, \mathrm{d}\mathbf{x}$$

and

$$\int_\Omega \nabla \cdot (\mathbf{K}_m \nabla\Psi_m)\, \varphi_m\, \mathrm{d}\mathbf{x} = \int_{\Sigma_N} \Psi_{N_m}\, \varphi_m\, \mathrm{d}S - \int_\Omega (\mathbf{K}_m \nabla\Psi_m) \cdot \nabla\varphi_m\, \mathrm{d}\mathbf{x}.$$

Let us define the following forms:

$$(u,v) = \int_\Omega uv\, \mathrm{d}\mathbf{x}, \quad u,v \in L^2(\Omega),$$

$$a_f(u,v) = \int_\Omega (\mathbf{K}_f(u-z)\nabla u) \cdot \nabla v\, \mathrm{d}\mathbf{x}, \quad u,v \in H^1(\Omega),$$

$$a_m(u,v) = \int_\Omega (\mathbf{K}_m(u-z)\nabla u) \cdot \nabla v\, \mathrm{d}\mathbf{x}, \quad u,v \in H^1(\Omega),$$

$$(u,v)_N = \int_{\partial\Omega_N} uv\, \mathrm{d}S, \quad u,v \in L^2(\partial\Omega_N).$$

Using the introduced notation, we can finally state the weak formulation of the problem (1.10).

Definition 1. *Pair of functions Ψ_f, Ψ_m is called a weak solution of problem 2.1, if it satisfies following conditions:*

$$\Psi_f - \Psi^* \in L^2(0, T; V_D), \quad \Psi_f \in L^\infty(Q),$$
$$\Psi_m - \Psi^{**} \in L^2(0, T; V_D), \quad \Psi_m \in L^\infty(Q),$$

where Ψ^* and Ψ^{**} are from (2.5),

$$\left(\gamma_f \frac{\partial \Psi_f(t)}{\partial t}, \varphi_f\right) + a_f(\Psi_f(t), \varphi_f) + \left(\frac{\Gamma_w(\Psi_f(t), \Psi_m(t))}{w_f}, \varphi_f\right) = (\Psi_{N_f}(t), \varphi_f)_N,$$
$$\left(\gamma_m \frac{\partial \Psi_m(t)}{\partial t}, \varphi_m\right) + a_m(\Psi_m(t), \varphi_m) - \left(\frac{\Gamma_w(\Psi_f(t), \Psi_m(t))}{w_m}, \varphi_m\right) = (\Psi_{N_m}(t), \varphi_m)_N$$

for all $\varphi_f, \varphi_m \in V_D$, and

$$\Psi_f(x, t = 0) = \Psi_{f_0} \quad in\ \Omega,$$
$$\Psi_m(x, t = 0) = \Psi_{m_0} \quad in\ \Omega.$$

The existence and uniqueness of the weak solution for the Richards equation was studied in [8] and [9]. However, for the non-linear Richards equation, as is our case, the question of the existence and uniqueness is open. We will assume that the weak solution exists and further we will not be concerned about it.

3. Numerical solution of Richards equation

In this chapter we present an approach to solve the Richards equation. Following [10], we approximate both spatial and temporal derivatives by the discontinuous Galerkin method (DGM). Section 3.1 introduces the notation and defines the key terms for DGM. Section 3.2 focuses on space discretization. The methodology of fully space-time discretization is presented in Section 3.3, where we also define the space-time discontinuous Galerkin approximate solution of the Richards equation. The solution yields the system of nonlinear algebraic equations, whose linearization is treated in Section 3.4. We present a Newton-like method for solving the mentioned system. Finally, we will discuss the stopping criteria for the solvers in Section 3.5 and lastly we mention a mesh adaptation in Section 3.6.

3.1 Assumptions, definitions and notations

Partition of the domain

Let $h > 0$ be a positive parameter and $\overline{\Omega}$ be a closure of the domain Ω. We define the partition $\mathcal{T}_h$ of $\overline{\Omega}$ as a finite number of closed triangles K with mutually disjoint interiors, such that

$$\overline{\Omega} = \bigcup_{K \in \mathcal{T}_h} K.$$

We call $\mathcal{T}_h$ a triangulation of the domain Ω. Further, we denote

- ∂K the boundary of a triangle $K \in \mathcal{T}_h$,

- h_k the diameter of K,

- $h = \max_{K \in \mathcal{T}_h} h_K$,

- ρ_K the radius of the largest circle inscribed into K,

- Γ the face of K,

- h_Γ the quantity representing the length of the face Γ.

The quantity h_Γ can be defined in many ways. We will use

$$h_\Gamma = \begin{cases} \frac{1}{2}\left(h_{K_\Gamma^L} + h_{K_\Gamma^R} \right) & \text{for } \Gamma \in \mathcal{F}_h^I, \\ h_{K_\Gamma^L} & \text{for } \Gamma \in \mathcal{F}_h^B. \end{cases} \tag{3.1}$$

By $|K|$ we denote the area of K and by $|\Gamma|$ we denote the length of Γ.

Let $K_1, K_2 \in T_h \subset \mathbb{R}^2$. Elements K_1 and K_2 are called neighbours, if their intersection $K_1 \cap K_2$ has positive 1-dimensional measure.

Let $\mathcal{F}_h$ denotes the system of all faces of all elements K in $\mathcal{T}_h$. We define the following sets:

- set of all boundary faces $\mathcal{F}_h^B = \{\Gamma \in \mathcal{F}_h : \Gamma \subset \partial\Omega\}$,

- set of all Dirichlet boundary faces $\mathcal{F}_h^D = \{\Gamma \in \mathcal{F}_h : \Gamma \subset \partial\Omega_D\}$,

- set of all Neumann boundary faces $\mathcal{F}_h^N = \{\Gamma \in \mathcal{F}_h : \Gamma \subset \partial\Omega_N\}$,

- set of all inner faces $\mathcal{F}_h^I = \mathcal{F}_h \setminus \mathcal{F}_h^B$.

For each $\Gamma \in \mathcal{F}_h$, we define a unit normal vector $\mathbf{n}_\Gamma$. If $\Gamma \in \mathcal{F}_h^B$, then $\mathbf{n}_\Gamma$ is the outer normal. The orientation of $\mathbf{n}_\Gamma$, $\Gamma \in \mathcal{F}_h^I$, is arbitrary, but fixed.

Assumptions on meshes

Let us consider the system of triangulations $\{\mathcal{T}_h\}_{h\in(0,\overline{h})}, \overline{h} > 0$, of the domain Ω. Then, we assume that

- the system $\{\mathcal{T}_h\}_{h\in(0,\overline{h})}$ is shape-regular, i.e.,

$$\exists\, C_R > 0 : \frac{h_K}{\rho_K} \leq C_R \quad \forall\, K \in \mathcal{T}_h \quad \forall\, h \in (0,\overline{h}),$$

where C_R is a positive constant,

- the equivalence condition holds, i.e., for each quantity h_Γ

$$\exists\, C_T, C_G > 0 : \; C_T h_K \leq h_\Gamma \leq C_G h_K \quad \forall\, K \in \mathcal{T}_h, \quad \forall\, \Gamma \in \mathcal{F}_h, \Gamma \subset \partial K,$$

where C_T, C_G are constants independent of h, K and Γ.

Spaces for DGM

To introduce the discontinuous Galerkin method, we need to define the space, where the approximate solution will be sought. For the triangulation $\mathcal{T}_h$ and any $k \in \mathbb{N}$, we define the broken Sobolev space

$$H^k(\Omega, \mathcal{T}_h) = \{v \in L^2(\Omega); v|_K \in H^k(K) \quad \forall\, K \in \mathcal{T}_h\}.$$

This space consists of functions, which are generally discontinuous on inner faces of elements $K \in T_h$. We further define the norms

$$\|v\|_{H^k(\Omega,\mathcal{T}_h)} = \left(\sum_{K\in\mathcal{T}_h} \|v\|_{H^k(K)^2} \right)^{1/2} \quad \text{for } v \in H^k(\Omega, \mathcal{T}_h),$$

$$|v|_{H^k(\Omega,\mathcal{T}_h)} = \left(\sum_{K\in\mathcal{T}_h} |v|_{H^k(K)^2} \right)^{1/2} \quad \text{for } v \in H^k(\Omega, \mathcal{T}_h).$$

Let $\Gamma \in F_h^I$ and $K_\Gamma^{(L)}, K_\Gamma^{(R)}$ be two neighbouring elements that share this face Γ, such that $\Gamma \subset \partial K_\Gamma^{(R)} \cap \partial K_\Gamma^{(L)}$. We define the trace, the mean values and the jumps for $v \in H^k(\Omega, \mathcal{T}_h)$ as

$v_\Gamma^{(L)} = $ the trace of $v|_{K_\Gamma^{(L)}}$ on Γ,

$v_\Gamma^{(R)} = $ the trace of $v|_{K_\Gamma^{(R)}}$ on Γ,

$\langle v \rangle_\Gamma = \frac{1}{2}\left(v_\Gamma^{(L)} + v_\Gamma^{(R)} \right)$ representing the mean value of the traces of v on Γ,

$[v]_\Gamma = v_\Gamma^{(L)} - v_\Gamma^{(R)}$ representing the jump of v on Γ.

For the boundary faces $\Gamma \in \mathcal{F}_h^B$, $\Gamma \subset \partial K_\Gamma^{(L)} \cup \partial\Omega$, we define

$$v_\Gamma^{(L)} = \text{the trace of } v|_{K_\Gamma^{(L)}} \text{ on } \Gamma,$$

$$\langle v \rangle_\Gamma = [v]_\Gamma = v_\Gamma^{(L)},$$

for $v \in H^k(\Omega, \mathcal{T}_h)$

Finally, for the triangulation $\mathcal{T}_h$ of Ω, let $p \geq 0$, $p \in \mathbb{N}$, and let us define the space of discontinuous piecewise polynomial functions

$$S_{hp} = \{v \in L^2(\Omega); v|_K \in P_p(K) \quad \forall K \in \mathcal{T}_h\},$$

where $P_p(K)$ denotes the space of all polynomials of degree $\leq p$ on K. It holds that $S_{hp} \subset H^k(\Omega, \mathcal{T}_h)$ for $k \leq 1$.

3.2 Space semi-discretization

Let us introduce the space discontinuous Galerkin discretization of the problem (2.1). For simplicity, we will derive the discretization with one equation using the index α, $\alpha \in \{f, m\}$, denoting the equation for the fracture and the matrix equations, respectively. Finally, we formulate the space semi-discrete solution in the vector form. We denote $\Gamma_f = -\Gamma_w/w_f$ and $\Gamma_m = \Gamma_w/w_m$.

Let us assume that

$$\boldsymbol{\Psi} = \begin{pmatrix} \Psi_f \\ \Psi_m \end{pmatrix} \in L^2(0, T; H^2(\Omega))^2, \quad \frac{\partial \boldsymbol{\Psi}(t)}{\partial t} \in (L^2(0, T; H^1(\Omega)))^2, \quad (3.2)$$

is the solution of (2.1) and let $\boldsymbol{\varphi} = (\varphi_f, \varphi_m)^T \in (H^2(\Omega, \mathcal{T}_h))^2$. We multiply (2.1) by $\boldsymbol{\varphi}$, integrate over $K \in \mathcal{T}_h$, use the Green's theorem and summing up over all elements $K \in \mathcal{T}_h$. We obtain

$$\sum_{K \in \mathcal{T}_h} \int_K \gamma_\alpha \frac{\partial \Psi_\alpha(t)}{\partial t} \varphi_\alpha \, d\mathbf{x} + \sum_{K \in \mathcal{T}_h} \int_K (\mathbf{K}_\alpha \nabla \Psi_\alpha(t)) \cdot \nabla \varphi_\alpha \, d\mathbf{x}$$
$$- \sum_{K \in \mathcal{T}_h} \int_{\partial K} (\mathbf{K}_\alpha \nabla \Psi_\alpha(t)) \cdot \mathbf{n}_K \varphi_\alpha \, dS = \sum_{K \in \mathcal{T}_h} \int_K \Gamma_\alpha(t) \varphi_\alpha \, d\mathbf{x}. \quad (3.3)$$

Since φ_α is in $H^2(K)$, the derivatives have the trace on ∂K and therefore the surface integrals are well defined. Let us now rewrite the surface integrals in the following way:

$$\sum_{K \in \mathcal{T}_h} \int_{\partial K} (\mathbf{K}_\alpha \nabla \Psi_\alpha(t)) \cdot \mathbf{n}_K \varphi_\alpha \, dS$$

$$= \sum_{\Gamma \in \mathcal{F}_h^D} \int_\Gamma (\mathbf{K}_\alpha \nabla \Psi_\alpha(t)) \cdot \mathbf{n}_\Gamma \varphi_\alpha \, dS + \sum_{\Gamma \in \mathcal{F}_h^N} \int_\Gamma (\mathbf{K}_\alpha \nabla \Psi_\alpha(t)) \cdot \mathbf{n}_\Gamma \varphi_\alpha \, dS$$

$$+ \sum_{\Gamma \in \mathcal{F}_h^I} \int_\Gamma \left((\mathbf{K}_\alpha \nabla \Psi_\alpha(t))_\Gamma^{(L)} (\varphi_\alpha)_\Gamma^{(L)} - (\mathbf{K}_\alpha \nabla \Psi_\alpha(t))_\Gamma^{(R)} (\varphi_\alpha)_\Gamma^{(R)} \right) \cdot \mathbf{n}_\Gamma \, dS.$$

Note that if $\mathbf{n}_\Gamma$ is the outer unit normal to $K_\Gamma^{(L)}$, then $\mathbf{n}_\Gamma$ is the inner unit normal to $K_\Gamma^{(R)}$ and therefore $-\mathbf{n}_\Gamma$ is the outer unit normal to $K_\Gamma^{(R)}$.

Since $\Psi_\alpha \in L^2(0, T; H^2(\Omega))$, Ψ_α and its derivatives are continuous over the inner faces, we can write

$$[\mathbf{K}_\alpha \nabla \Psi_\alpha(t)]_\Gamma = 0 \Leftrightarrow (\mathbf{K}_\alpha \nabla \Psi_\alpha(t))_\Gamma^{(L)} = (\mathbf{K}_\alpha \nabla \Psi_\alpha(t))_\Gamma^{(R)} \qquad \forall \Gamma \in \mathcal{F}_h^I,$$

$$\langle \mathbf{K}_\alpha \nabla \Psi_\alpha(t) \rangle_\Gamma = (\mathbf{K}_\alpha \nabla \Psi_\alpha(t))_\Gamma^{(L)} = (\mathbf{K}_\alpha \nabla \Psi_\alpha(t))_\Gamma^{(R)} \qquad \forall \Gamma \in \mathcal{F}_h^I.$$

Thus, we can express the surface integrand over the inner faces as

$$\left((\mathbf{K}_\alpha \nabla \Psi_\alpha(t))_\Gamma^{(L)} (\varphi_\alpha)_\Gamma^{(L)} - (\mathbf{K}_\alpha \nabla \Psi_\alpha(t))_\Gamma^{(R)} (\varphi_\alpha)_\Gamma^{(R)} \right) \cdot \mathbf{n}_\Gamma = \langle \mathbf{K}_\alpha \nabla \Psi_\alpha(t) \rangle_\Gamma \cdot \mathbf{n}_\Gamma \, [\varphi_\alpha]_\Gamma.$$

The integrand over the Dirichlet boundary faces can be rewritten as

$$(\mathbf{K}_\alpha \nabla \Psi_\alpha(t)) \cdot \mathbf{n}_\Gamma \, \varphi_\alpha = \langle \mathbf{K}_\alpha \nabla \Psi_\alpha(t) \rangle_\Gamma \cdot \mathbf{n}_\Gamma \, [\varphi_\alpha]_\Gamma,$$

since for the boundary faces Γ holds

$$(\mathbf{K}_\alpha \nabla \Psi_\alpha(t)) = \langle \mathbf{K}_\alpha \nabla \Psi_\alpha(t) \rangle_\Gamma$$

and

$$\varphi_\alpha = [\varphi_\alpha]_\Gamma.$$

Altogether, substituing the Neumann boundary condition, we can rewrite the surface integral as

$$\sum_{K \in \mathcal{T}_h} \int_{\partial K} (\mathbf{K}_\alpha \nabla \Psi_\alpha(t)) \cdot \mathbf{n}_K \, \varphi_\alpha \, \mathrm{d}S$$
$$= \int_{\Sigma_N} \Psi_{N_\alpha}(t) \, \varphi_\alpha \, \mathrm{d}S + \sum_{\Gamma \in \mathcal{F}_h^{ID}} \int_\Gamma \langle \mathbf{K}_\alpha \nabla \Psi_\alpha(t) \rangle_\Gamma \cdot \mathbf{n}_\Gamma \, [\varphi_\alpha]_\Gamma \, \mathrm{d}S. \tag{3.4}$$

Using (3.4), we can rewrite the identity (3.3) as

$$\int_\Omega \gamma_\alpha \frac{\partial \Psi_\alpha(t)}{\partial t} \, \varphi_\alpha \, \mathrm{d}\mathbf{x} + \sum_{K \in \mathcal{T}_h} \int_K (\mathbf{K}_\alpha \nabla \Psi_\alpha(t)) \cdot \nabla \varphi_\alpha \, \mathrm{d}\mathbf{x}$$
$$- \sum_{\Gamma \in \mathcal{F}_h^{ID}} \int_\Gamma \langle \mathbf{K}_\alpha \nabla \Psi_\alpha(t) \rangle_\Gamma \cdot \mathbf{n}_\Gamma \, [\varphi_\alpha]_\Gamma \, \mathrm{d}S = \int_{\Sigma_N} \Psi_{N_\alpha}(t) \, \varphi_\alpha \, \mathrm{d}S + \int_\Omega \Gamma_\alpha(t) \, \varphi_\alpha \, \mathrm{d}\mathbf{x}. \tag{3.5}$$

To ensure the existence of the approximate solution, we must include additional terms in our formulation (3.5). We define the interior and the boundary penalty bilinear form

$$J_h^\sigma(u, v) = \sum_{\Gamma \in \mathcal{F}_h^I} \int_\Gamma \sigma [u]_\Gamma [v]_\Gamma \, \mathrm{d}S + \sum_{\Gamma \in \mathcal{F}_h^D} \int_\Gamma \sigma u v \, \mathrm{d}S$$
$$= \sum_{\Gamma \in \mathcal{F}_h^{ID}} \int_\Gamma \sigma [u]_\Gamma [v]_\Gamma \, \mathrm{d}S, \quad u, v \in H^2(\Omega, \mathcal{T}_h),$$

where $\sigma > 0$ is the penalty weight. We will consider the penalty weight in the form

$$\sigma : \cup_{\Gamma \in \mathcal{F}_h^{ID}} \to \mathbb{R},$$

$$\sigma|_\Gamma = \sigma_\Gamma = \frac{C_W}{h_\Gamma}, \quad \Gamma \in \mathcal{F}_h^{ID},$$

where C_W is the penalization constant and h_Γ is defined in (3.1). Further, we define the boundary linear form as

$$J_D^\sigma(v) = \sum_{\Gamma \in \mathcal{F}_h^D} \int_\Gamma \sigma \Psi_{D_\alpha} v \, \mathrm{d}S, \quad v \in H^2(\Omega, \mathcal{T}_h),$$

where Ψ_{D_α} is the Dirichlet boundary condition defined in (2.2). Note that if $\Psi_\alpha \in L^2(0, T; H^2(\Omega))$ is the solution of (3.5), then

$$J_h^\sigma(\Psi_\alpha, v) = J_D^\sigma(v) \quad \forall v \in H^2(\Omega, \mathcal{T}_h). \tag{3.6}$$

We impose the continuity of the approximate solution on the interior faces by adding the interior and the boundary penalty into our formulation.

Moreover, we will use the -1, 1 or 0-multiple of the identity

$$\sum_{\Gamma \in \mathcal{F}_h^{ID}} \int_\Gamma \langle \mathbf{K}_\alpha(\Psi_\alpha - z)\nabla v \rangle_\Gamma \cdot \mathbf{n}_\Gamma \, [\Psi_\alpha]_\Gamma \, \mathrm{d}S = \sum_{\Gamma \in \mathcal{F}_h^D} \int_\Gamma \mathbf{K}_\alpha(\Psi_\alpha - z)\nabla v \cdot \mathbf{n}_\Gamma \, \Psi_{D_\alpha} \, \mathrm{d}S,$$

$$\forall v \in H^2(\Omega, \mathcal{T}_h),$$

to add to the right-hand side of (3.5). This leads to the definition of the following forms: For $u, v, f, g \in H^2(\Omega, \mathcal{T}_h)$, we define the forms

$$
\begin{aligned}
a_{\alpha,h}(u, v, f, g) = & \sum_{K \in T_h} \int_K (\mathbf{K}_\alpha(u - z)\nabla u) \cdot \nabla v \, \mathrm{d}\mathbf{x} \\
& - \sum_{\Gamma \in \mathcal{F}_h^{ID}} \int_\Gamma \left(\langle \mathbf{K}_\alpha(u - z)\nabla u \rangle_\Gamma \cdot \mathbf{n}_\Gamma \, [v]_\Gamma + \Theta \langle \mathbf{K}_\alpha(u - z)\nabla v \rangle_\Gamma \cdot \mathbf{n}_\Gamma \, [u]_\Gamma \right) \mathrm{d}S \\
& + \Theta \sum_{\Gamma \in \mathcal{F}_h^D} \int_\Gamma \mathbf{K}_\alpha(u - z)\nabla v \cdot \mathbf{n}_\Gamma \, \Psi_{D_\alpha} \, \mathrm{d}S \\
& - \int_\Omega \Gamma_w(f, g) \, v \, \mathrm{d}\mathbf{x} - \int_{\Sigma_N} \Psi_{N_\alpha} \, v \, \mathrm{d}S,
\end{aligned}
\tag{3.7}
$$

where $\Theta \in \{-1, 0, 1\}$, $\alpha \in \{f, m\}$.

Therefore, we can write (3.3) as

$$\left(\gamma_\alpha(\Psi_\alpha(t) - z) \frac{\partial \Psi_\alpha(t)}{\partial t}, \varphi_\alpha \right) + a_{\alpha,h}(\Psi_\alpha(t), \varphi_\alpha, \Psi_f(t), \Psi_m(t)) = 0 \tag{3.8}$$

for φ_α in $H^2(\Omega, \mathcal{T}_h)$, $\alpha \in \{f, m\}$.

Adding the penalty terms from (3.6) to the equality (3.8) yields the definition of the discontinuous Galerkin weak formulation. As we advised, we formulate it in the vector form. For $\boldsymbol{U} = (U_f, U_m)^T \in (H^2(\Omega, \mathcal{T}_h))^2$ we define the vector variant of the form $a_{\alpha,h}$ and of the boundary penalty terms as follows:

$$\boldsymbol{a}_h(\boldsymbol{U}, \boldsymbol{\varphi}, U_f, U_m) = \begin{pmatrix} a_{f,h}(U_f, \varphi_f, U_f, U_m) \\ a_{m,h}(U_m, \varphi_m, U_f, U_m) \end{pmatrix},$$

$$\boldsymbol{J}_h^\sigma(\boldsymbol{U}, \boldsymbol{\varphi}) = \begin{pmatrix} J_h^\sigma(U_f, \varphi_f) \\ J_h^\sigma(U_m, \varphi_m) \end{pmatrix}, \quad \boldsymbol{J}_D^\sigma(\boldsymbol{\varphi}) = \begin{pmatrix} J_D^\sigma(\varphi_f) \\ J_D^\sigma(\varphi_m) \end{pmatrix}.$$

Definition 2. *Function* $\boldsymbol{U} = (U_f, U_m)^T : Q^2 \to \mathbb{R}^2$ *is called a discontinuous Galerkin semidiscrete approximate solution of the problem* (2.1), *if it satisfies*

$$\boldsymbol{U} \in (C^1([0,T]; S_{hp}))^2$$

and one of the following identities

$$\left(\boldsymbol{\gamma}(\boldsymbol{U}(t) - \boldsymbol{z})\frac{\partial \boldsymbol{U}(t)}{\partial t}, \boldsymbol{\varphi}\right) + \boldsymbol{a}_h(\boldsymbol{U}(t), \boldsymbol{\varphi}, U_f(t), U_m(t))$$
$$+ \boldsymbol{J}_h^\sigma(\boldsymbol{U}(t), \boldsymbol{\varphi}) - \boldsymbol{J}_D^\sigma(\boldsymbol{\varphi}) = 0 \quad \forall \boldsymbol{\varphi} \in (S_{hp})^2, \tag{3.9}$$

with

$$\begin{pmatrix} (U_{f,0}, \varphi_f) \\ (U_{m,0}, \varphi_m) \end{pmatrix} = \begin{pmatrix} (\Psi_{f_0}, \varphi_f) \\ (\Psi_{m_0}, \varphi_m) \end{pmatrix} \quad \forall (\varphi_f, \varphi_m)^T \in (S_{hp})^2,$$

holds for $\Theta \in \{-1, 0, 1\}$, *where* Ψ_{f_0}, Ψ_{m_0} *are defined in* (2.4) *and*

$$\left(\boldsymbol{\gamma}(\boldsymbol{U}(t) - \boldsymbol{z})\frac{\partial \boldsymbol{U}(t)}{\partial t}, \boldsymbol{\varphi}\right) = \begin{pmatrix} \left(\gamma_f(U_f - z)\frac{\partial U_f(t)}{\partial t}, \varphi_f\right) \\ \left(\gamma_m(U_m - z)\frac{\partial U_m(t)}{\partial t}, \varphi_m\right) \end{pmatrix}$$

The definition 2 introduces the three variants of the discretization of the diffusion terms: $\Theta = -1, 0, 1$ stands for non-symmetric, incomplete and symmetric variant, respectively.

3.3 Space-time discretization

The previous section covered only the discontinuous Galerkin discretization with respect to the space. In this section, we introduce the fully space-time discontinuous Galerkin discretization of the problem (2.1). We employ the same notation as was introduced in the previous section, we only add a subscript $_k$ for the time discretization.

Let $r > 0$ be an integer and $T > 0$ the end time. We construct the partition $0 = t_0 < \ldots < t_r = T$ of the time interval $[0, T]$ and denote the subintervals

$$I_k = (t_{k-1}, t_k), \quad \overline{I}_k = [t_{k-1}, t_k], \quad k = 1, \ldots, r,$$

and

$$\tau_k = t_k - t_{k-1}, \quad \tau = \max_{k=1,\ldots,r} \tau_k.$$

Then

$$[0, T] = \cup_{k=1}^r \overline{I}_k, \quad I_k \cap I_n = \emptyset \quad \text{for } k \neq n, \ k, n = 1, \ldots, r.$$

Thus, $\mathcal{T}_{h,k}$ denotes a triangulation on the time level I_k. For every time interval I_k, $k = 1, \ldots, r$, the space partition $\mathcal{T}_{h,k}$ of Ω is different in general.

Further, we introduce the following notation: Let φ be a function defined in $\cup_{k=1}^r I_k$ and let us assume that one-sided limits

$$\lim_{t \to t_k^\pm} \varphi(t)$$

18

exist. We define

$$\varphi_k^{\pm} := \varphi(t_k^{\pm}) = \lim_{t \to t_k^{\pm}} \varphi(t) \tag{3.10}$$

and the jump with respect to the time on the time level I_k

$$\{\varphi\}_k = \varphi_k^+ - \varphi_k^-.$$

We consider a varying polynomial degree with respect to the space, i.e., for each triangle $K \in \mathcal{T}_{h,k}$ we denote a positive number p_K as a polynomial degree on K. Then we define the finite-dimensional space

$$S_{h,p,k} = \{\varphi \in L^2(\Omega); \varphi|_K \in P^{p_K}(K) \quad \forall K \in \mathcal{T}_{h,k}\}.$$

Moreover, we consider a fixed polynomial degree $q \in \mathbb{N}$ in time and we define the space of the functions piecewise polynomial in space and time

$$S_{h,\tau}^{p,q} = \{\varphi \in L^2(Q); \ \varphi(x,t)|_{I_k} = \sum_{i=0}^{q} t^i \, \varphi_{k,i}(x),$$

$$\varphi_{k,i} \in S_{h,p,k}, i = 0, \dots, q, k = 1, \dots, r\}.$$

Remark 2. If $\varphi \in S_{h,\tau}^{p,q}$, then $\varphi|_{K \times I_k}$ is a polynomial with degree $\le p_K$ with respect to the space and with degree $\le q$ with respect to the time. This means

$$\varphi|_{K \times I_k} \in P^{p_K}(K) \times P^q(I_k) \iff \varphi|_{K \times I_k}(x,t) = \sum_{i,j=0}^{i+j \le p_K} \sum_{k=0}^{q} \alpha_{ijk} x_1^i x_2^j t^k,$$

$$\alpha_{ijk} \in \mathbb{R}, x = (x_1, x_2) \in K, t \in I_k.$$

We consider again the exact solution

$$\boldsymbol{\Psi} = \begin{pmatrix} \Psi_f \\ \Psi_m \end{pmatrix} \in L^2(0,T; H^2(\Omega))^2, \quad \frac{\boldsymbol{\Psi}(t)}{\partial t} \in (L^2(0,T; H^1(\Omega)))^2,$$

of the problem (2.1) and the test function $\boldsymbol{\varphi} = (\varphi_f, \varphi_m)^T \in (S_{h,\tau}^{p,q})^2$. It also holds that $\boldsymbol{\Psi} \in C([0,T]; H^1(\Omega))^2$. Let $k \in \{1, \dots, r\}$ be arbitrary (but fixed) and denote $\Psi'_\alpha = \partial \Psi_\alpha / \partial t$, $\alpha \in \{f, m\}$. We multiply equation (2.1) by $\varphi_\alpha \in S_{h,\tau}^{p,q}$, integrate over $K \times I_k$ and sum up over all elements $K \in \mathcal{T}_{h,k}$. Then

$$\int_{I_k} (\gamma_\alpha \Psi'_\alpha, \varphi_\alpha) \, \mathrm{d}t - \int_{I_k} \underbrace{\int_K \nabla \cdot (\mathbf{K}_\alpha \nabla \Psi_\alpha) \, \varphi_\alpha \, \mathrm{d}\mathbf{x}}_{(*)} \, \mathrm{d}t = \int_{I_k} (\Gamma_\alpha, \varphi_\alpha) \, \mathrm{d}t.$$

We dealt with term $(*)$ in the previous chapter, so it remains to handle the term with the time derivation. For better manipulation, we write $\frac{\partial \vartheta_\alpha(\Psi_\alpha - z)}{\partial t}$ instead of $\gamma_\alpha \Psi'_\alpha$. We use the integration by parts with respect to the time for the term with the time derivation as follows:

$$\int_{I_k} \left(\frac{\partial \vartheta_\alpha(\Psi_\alpha - z)}{\partial t}, \varphi_\alpha \right) \mathrm{d}t = -\int_{I_k} (\vartheta_\alpha(\Psi_\alpha - z), \varphi'_\alpha) \, \mathrm{d}t$$

$$+ (\vartheta_\alpha(\Psi_{\alpha,k}^- - z_k^-), \varphi_{\alpha,k}^-) - (\vartheta_\alpha(\Psi_{\alpha,k-1}^+ - z_{k-1}^+), \varphi_{\alpha,k-1}^+), \tag{3.11}$$

19

and since Ψ_α and z are continuous in time, we have (cf. (3.10))

$$\vartheta_\alpha(\Psi^+_{\alpha,k-1} - z^+_{k-1}) = \vartheta_\alpha(\Psi^-_{\alpha,k-1} - z^-_{k-1})$$

and thus

$$(\vartheta_\alpha(\Psi^+_{\alpha,k-1} - z^+_{k-1}), \varphi^+_{\alpha,k-1}) = (\vartheta_\alpha(\Psi^-_{\alpha,k-1} - z^-_{k-1}), \varphi^+_{\alpha,k-1}). \tag{3.12}$$

Once again using integration by parts and applying the identity (3.12), we obtain

$$
\begin{aligned}
\int_{I_k} \left(\frac{\partial \vartheta_\alpha(\Psi_\alpha - z)}{\partial t}, \varphi_\alpha \right) \mathrm{d}t &= \int_{I_k} \left(\frac{\partial \vartheta_\alpha(\Psi_\alpha - z)}{\partial t}, \varphi_\alpha \right) \mathrm{d}t \\
&\quad + (\vartheta_\alpha(\Psi^+_{\alpha,k-1} - z^+_{k-1}), \varphi^+_{\alpha,k-1}) - (\vartheta_\alpha(\Psi^-_{\alpha,k-1} - z^-_{k-1}), \varphi^+_{\alpha,k-1}) \\
&= \int_{I_k} \left(\frac{\partial \vartheta_\alpha(\Psi_\alpha - z)}{\partial t}, \varphi_\alpha \right) \mathrm{d}t + (\{\vartheta_\alpha(\Psi_\alpha - z)\}_{k-1}, \varphi^+_{\alpha,k-1}).
\end{aligned}
\tag{3.13}
$$

Thus the exact solution $\boldsymbol{\Psi} = (\Psi_f, \Psi_m)$ satisfies the identity

$$
\begin{aligned}
\int_{I_k} \left(\frac{\partial \vartheta_\alpha(\Psi_\alpha - z)}{\partial t}, \varphi_\alpha \right) + a_{\alpha,h,k}(\Psi_\alpha, \varphi_\alpha, \Psi_f, \Psi_m) + J^\sigma_{h,k}(\Psi_\alpha, \varphi_\alpha) \\
- J^\sigma_{D,k}(\varphi_\alpha) \, \mathrm{d}t + (\{\vartheta_\alpha(\Psi_\alpha - z\}_{k-1}, \varphi^+_{\alpha,k-1}) = 0 \quad \forall \varphi_\alpha \in S^{p,q}_{h,\tau}
\end{aligned}
\tag{3.14}
$$

with $\Psi_\alpha(0-) = \Psi_{\alpha_0}$, $\alpha \in \{f, m\}$.

Remark 3. Forms $a_{\alpha,h,k}$, $J^\sigma_{h,k}$ and $J_{D,k}$ in (3.14) are defined in the same manner as in the previous section. The difference is only in the range of the sum: here, we are summing over $K \in \mathcal{T}_{h,k}$ and $\Gamma \in \mathcal{F}_{h,k}$.

This process leading to equation (3.14) is the standard way to define a space-time discontinuous Galerkin approximation of the problem (2.1). However, treating the first term in (3.14) in a way

$$\left(\frac{\partial \vartheta_\alpha(\Psi_\alpha - z)}{\partial t}, \varphi_\alpha \right) = \left(\gamma_\alpha(\Psi_\alpha - z) \frac{\partial \Psi_\alpha}{\partial t}, \varphi_\alpha \right) \tag{3.15}$$

leads to some inaccuracy in the water content balance, due to the low regularity of ϑ_α, particularly $\vartheta'_\alpha(0)$ is discontinuous. Therefore, we will present a different approach of defining the approximate solution.

Substituting the identity (3.12) into (3.11) leads to

$$
\begin{aligned}
\int_{I_k} \left(\frac{\partial \vartheta_\alpha(\Psi_\alpha - z)}{\partial t}, \varphi_\alpha \right) \mathrm{d}t &= - \int_{I_k} (\vartheta_\alpha(\Psi_\alpha - z), \varphi'_\alpha) \, \mathrm{d}t \\
&\quad + (\vartheta_\alpha(\Psi^-_{\alpha,k} - z^-_k), \varphi^-_{\alpha,k}) - (\vartheta_\alpha(\Psi^-_{\alpha,k-1} - z^-_{k-1}), \varphi^+_{\alpha,k-1}),
\end{aligned}
$$

where $\varphi'_\alpha = \partial \varphi_\alpha / \partial t$.

Finally, we can define the form $A_{\alpha,h,k} : S^{p,q}_{h,\tau} \times S^{p,q}_{h,\tau} \times S^{p,q}_{h,\tau} \times S^{p,q}_{h,\tau} \to \mathbb{R}$ as

$$
\begin{aligned}
A_{\alpha,h,k}(u, v, f, g) &= \int_{I_k} -(\vartheta_\alpha(u - z), v') + a_{\alpha,h,k}(u, v, f, g) \\
&\quad + J^\sigma_{h,k}(u, v) - J^\sigma_{D,k}(v) \, \mathrm{d}t \\
&\quad + (\vartheta_\alpha(u^-_k - z^-_k), v^-_k) - (\vartheta_\alpha(u^-_{k-1} - z^-_{k-1}), v^+_{k-1})
\end{aligned}
\tag{3.16}
$$

for $u, v, f, g \in S^{p,q}_{h,\tau}$. The last term in the equation (3.16) establishes a connection between the approximations of the two consecutive time layers.

We can now proceed to the definition of the approximate solution.

Definition 3. *Function $\boldsymbol{U} = (U_f, U_m)^T : Q^2 \to \mathbb{R}^2$ is called a space-time discontinuous Galerkin approximate solution of the problem (2.1), if $\boldsymbol{U} \in (S_{h,\tau}^{p,q})^2$ and $\boldsymbol{U}$ satisfies the following identity*

$$\boldsymbol{A}_{h,k}(\boldsymbol{U}, \boldsymbol{\varphi}) = 0 \quad \forall \, \boldsymbol{\varphi} \in (S_{h,\tau}^{p,q})^2, \, k = 1, \dots, r, \tag{3.17}$$

with $(U_{f_0}^-, U_{m_0}^-)^T = (\Psi_{f_0}, \Psi_{m_0})^T$ given by the initial condition 2.4, where the form $\boldsymbol{A}_{h,k} : (S_{h,\tau}^{p,q})^2 \times (S_{h,\tau}^{p,q})^2 \to \mathbb{R}^2$ is defined as

$$\boldsymbol{A}_{h,k}(\boldsymbol{U}, \boldsymbol{\varphi}) = \begin{pmatrix} A_{f,h,k}(U_f, \varphi_f, U_f, U_m) \\ A_{m,h,k}(U_m, \varphi_m, U_f, U_m) \end{pmatrix}.$$

Notice, that the space $(S_{h,\tau}^{p,q})^2$, where the approximate solution is sought, is independent of the boundary conditions and that the components U_f, U_m are connected through the exchange term Γ_w.

The existence and the uniqueness of the approximate solution for single Richards equation has been proved for the linear case in [10]. However, the existence and the uniqueness for the general nonlinear Richards equation with a dual-permeability model is open.

3.4 Solution strategy

The definition of the approximate solution in (3.17) is equivalent to the system of nonlinear algebraic equations for each time level $k = 1, \dots, r$. According to Remark 2, each system in (3.17) consist of $2N_k$ equations, where the number $N_k = (q+1)\sum_{K \in \mathcal{T}_{h,k}}(p_K+1)(p_K+2)/2$ (if $\Omega \subset \mathbb{R}^2$), where p_K is a polynomial approximation degree in space and q is a polynomial approximation degree in time. We call the number $2N_k$ the degree of freedom of the mesh $\mathcal{T}_{h,k}$.

We will follow the linearization technique presented in [2]. We define the space of piecewise polynomial functions on one time layer k

$$S_{h,\tau,k}^{p,q} := \{\varphi : \Omega \times I_k \to \mathbb{R}, \, \varphi|_{K \times I_k} \in P^{p_K}(K) \times P^q(I_k), K \in \mathcal{T}_{h,k}\}.$$

Let $\boldsymbol{\Psi} = (\Psi_f, \Psi_m)^T \in (S_{h,\tau}^{p,q})^2$ be the approximate solution of (3.17) and denote its restriction to the space $S_{h,\tau,k}^{p,q}$, $\boldsymbol{\Psi}^k := \boldsymbol{\Psi}|_{\Omega \times I_k}$. Further, we define a basis $B_{h,k}$ of the space $S_{h,\tau,k}^{p,q}$ as $B_{h,k} := \{\varphi_i(x,t)\}_{i=1}^{N_k}$, where N_k is the dimension of $S_{h,\tau,k}^{p,q}$. Let the basis $B_{h,k}$ be L^2 orthogonal and constructed as a composition of local bases for each $K \times I_k, K \in \mathcal{T}_{h,k}, I_k \in [0,T]$, i.e., each $K \times I_k$ has a corresponding basis function $\varphi_{K \times I_k}$ such that supp $\varphi_{K \times I_k} \subset K \times I_k$. Then we can express

$$\boldsymbol{\Psi}^k(x,t) = \begin{pmatrix} \Psi_f^k(x,t) \\ \Psi_m^k(x,t) \end{pmatrix} = \begin{pmatrix} \sum_{j=1}^{N_k} \xi_f^{k,j} \varphi_j(x,t) \\ \sum_{j=1}^{N_k} \xi_m^{k,j} \varphi_j(x,t) \end{pmatrix},$$

where $\xi_f^{k,j}, \xi_m^{k,j} \in \mathbb{R}, j = 1, \dots, N_k$, are the basis coefficients for the fracture component Ψ_f^k and the matrix component Ψ_m^k, respectively. Let us note, that we want to express both components with respect to the basis $B_{h,k}$. Therefore, the basis of space $(S_{h,\tau,k}^{p,q})^2$, where the approximate solution on time level k is sought can be defined as

$$(B_{h,k})^2 := \left\{ \begin{pmatrix} \varphi_i \\ 0 \end{pmatrix}, \begin{pmatrix} 0 \\ \varphi_i \end{pmatrix} \right\}_{i=1}^{N_k} = \{\boldsymbol{\varphi}_i\}_{i=1}^{2N_k}. \tag{3.18}$$

21

From Definition 3 we have

$$\boldsymbol{A}_{h,k}(\boldsymbol{\Psi}^k, \boldsymbol{\varphi}_i) = 0, \quad , \quad i = 1, \ldots, 2N_k,$$

for

$$\boldsymbol{\varphi}_i = (\varphi_i, 0)^T, \quad i = 1, \ldots, N_k, \quad \boldsymbol{\varphi}_i = (0, \varphi_{N_k-i})^T \quad i = N_k + 1, \ldots, 2N_k,$$
$$k = 1, \ldots, r.$$

In order to reformulate the system (3.17), we define the vector valued function $\mathbf{F}_{h,k} : \mathbb{R}^{2N_k} \to \mathbb{R}^{2N_k}$ as

$$\mathbf{F}_{h,k}(\boldsymbol{\xi}^k) := \{\boldsymbol{A}_{h,k}(\boldsymbol{\Psi}^k, \boldsymbol{\varphi}_i)\}_{i=1}^{2N_k}, \quad k = 1, \ldots, r,$$

where $\boldsymbol{\xi}^k = (\xi_f^{k,1}, \ldots, \xi_f^{k,N_k}, \xi_m^{k,1}, \ldots, \xi_m^{k,N_k})$ and the scalars $\xi_f^{k,j}$, $\xi_m^{k,j}$, $j = 1, \ldots, N_k$, are the coordinates of the approximate solution Ψ_f^k, Ψ_m^k, respectively, with respect to the basis $B_{h,k}$.

Note, that from the definition of the form $A_{\alpha,h,k}$ (3.16), we see that the function $\mathbf{F}_{h,k}$ also depends on $\boldsymbol{\Psi}^{k-1}$. Thus, the system of nonlinear algebraic equation (3.17) can be represented as:

$$\text{Find } \boldsymbol{\xi}^k \in \mathbb{R}^{2N_k} : \mathbf{F}_{h,k}(\boldsymbol{\xi}_k) = 0, \quad k = 1, \ldots, r. \tag{3.19}$$

Therefore, problem (3.19) is a root finding problem and we can use the famous Newton method to solve it. However, the Newton method for a vector valued function requires computing the Jacobian matrix

$$\mathbf{J}_{h,k}(\boldsymbol{\xi}) := \frac{\mathrm{d}\mathbf{F}_{h,k}(\boldsymbol{\xi})}{\mathrm{d}\boldsymbol{\xi}},$$

which is usually a difficult task. Therefore, we will present a different approach: a linearization of the form $A_{\alpha,h,k}$ and then approximating the Jacobian matrix.

The system (3.19) is strongly nonlinear, therefore we need to perform a linearization of the form $A_{\alpha,h,k}$. First, we need to deal with the time derivative term. For $\alpha \in \{f, m\}$, we express this term as derived in (3.13) and (3.15),

$$\int_{I_k} \left(\frac{\partial \vartheta_\alpha(\Psi_\alpha - z)}{\partial t}, \varphi_\alpha \right) \mathrm{d}t$$
$$= \int_{I_k} \left(\gamma_\alpha(\Psi_\alpha - z) \frac{\partial \Psi_\alpha}{\partial t}, \varphi_\alpha \right) \mathrm{d}t + (\{\vartheta_\alpha(\Psi_\alpha - z)\}_{k-1}, \varphi_{\alpha,k-1}^+) \tag{3.20}$$
$$\approx \int_{I_k} \left(\gamma_\alpha(\Psi_\alpha - z) \frac{\partial \Psi_\alpha}{\partial t}, \varphi_\alpha \right) \mathrm{d}t + (\gamma_\alpha(\Psi_\alpha - z) \{\Psi_\alpha\}_{k-1}, \varphi_{\alpha,k-1}^+),$$

where the term $\{\vartheta_\alpha(\Psi_\alpha - z)\}_{k-1}$ is approximated as

$$\{\vartheta_\alpha(\Psi_\alpha - z)\}_{k-1} = \vartheta_\alpha(\Psi_\alpha - z)|_{k-1}^+ - \vartheta_\alpha(\Psi_\alpha - z)|_{k-1}^- = \int_{(\Psi_\alpha - z)|_{k-1}^-}^{(\Psi_\alpha - z)|_{k-1}^+} \vartheta_\alpha'(s) \, \mathrm{d}s$$
$$\approx \gamma_\alpha((\Psi_\alpha - z)|_{k-1}^+) \, (\Psi_\alpha|_{k-1}^+ - \Psi_\alpha|_{k-1}^-)$$
$$= \gamma_\alpha((\Psi_\alpha - z)|_{k-1}^+) \, \{\Psi_\alpha\}_{k-1}.$$

We introduce the linearization of forms $A_{\alpha,h,k}$, $\alpha \in \{f, m\}$, $k = 1, \ldots, r$. Let us define the forms

$$a_{f,h,k}^{L}(\Psi_f, \Psi_m, \varphi, \overline{\Psi_f}, \overline{\Psi_m}) = \sum_{K \in T_{h,k}} \int_K (\mathbf{K}_f(\overline{\Psi_f} - z)\nabla\Psi_f) \cdot \nabla\varphi \, \mathrm{d}\mathbf{x}$$

$$- \sum_{\Gamma \in \mathcal{F}_{h,k}^{ID}} \int_\Gamma \left(\langle \mathbf{K}_f(\overline{\Psi_f} - z)\nabla\Psi_f \rangle_\Gamma \cdot \mathbf{n}_\Gamma \, [\varphi]_\Gamma + \Theta \langle \mathbf{K}_f(\overline{\Psi_f} - z)\nabla\varphi \rangle_\Gamma \cdot \mathbf{n}_\Gamma \, [\Psi_f]_\Gamma \right) \mathrm{d}S$$

$$- \int_\Omega \Gamma_w(\Psi_f, \Psi_m, \overline{\Psi_f}, \overline{\Psi_m}) \, v \, \mathrm{d}\mathbf{x},$$

$$a_{m,h,k}^{L}(\Psi_m, \Psi_f, \varphi, \overline{\Psi_f}, \overline{\Psi_m}) = \sum_{K \in T_{h,k}} \int_K (\mathbf{K}_m(\overline{\Psi_m} - z)\nabla\Psi_m) \cdot \nabla\varphi \, \mathrm{d}\mathbf{x}$$

$$- \sum_{\Gamma \in \mathcal{F}_{h,k}^{ID}} \int_\Gamma \left(\langle \mathbf{K}_m(\overline{\Psi_m} - z)\nabla\Psi_m \rangle_\Gamma \cdot \mathbf{n}_\Gamma \, [\varphi]_\Gamma + \Theta \langle \mathbf{K}_m(\overline{\Psi_m} - z)\nabla\varphi \rangle_\Gamma \cdot \mathbf{n}_\Gamma \, [\Psi_m]_\Gamma \right) \mathrm{d}S$$

$$- \int_\Omega \Gamma_w(\Psi_f, \Psi_m, \overline{\Psi_f}, \overline{\Psi_m}) \, v \, \mathrm{d}\mathbf{x},$$

and

$$d_{\alpha,h,k}^{L}(\varphi, \overline{\Psi_\alpha}) = -\Theta \sum_{\Gamma \in \mathcal{F}_{h,k}^{D}} \int_\Gamma \mathbf{K}_\alpha(\overline{\Psi_\alpha} - z)\nabla\varphi \cdot \mathbf{n}_\Gamma \, \Psi_{D_\alpha} \, \mathrm{d}S + \int_{\Sigma_N} \Psi_{N_\alpha} \, \varphi \, \mathrm{d}S.$$

Recall the form of the exchange term to clarify its arguments:

$$\Gamma_w(\Psi_f, \Psi_m, \overline{\Psi_f}, \overline{\Psi_m}) = a_w(\overline{\Psi_f}, \overline{\Psi_m})\,(\Psi_m - \Psi_f).$$

Due to (3.7) and Remark 3, we have

$$a_{f,h,k}(\Psi_f, \varphi, \Psi_f, \Psi_m) = a_{f,h,k}^{L}(\Psi_f, \Psi_m, \varphi, \Psi_f, \Psi_m) - d_{f,h,k}^{L}(\varphi, \Psi_f)$$

$$a_{m,h,k}(\Psi_m, \varphi, \Psi_f, \Psi_m) = a_{m,h,k}^{L}(\Psi_m, \Psi_f, \varphi, \Psi_f, \Psi_m) - d_{m,h,k}^{L}(\varphi, \Psi_m)$$

$$\forall \, \Psi_m, \Psi_f, \varphi \in S_{h,\tau}^{p,q}.$$

Using (3.20), we define

$$A_{f,h,k}^{L}(\Psi_f, \Psi_m, \varphi, \overline{\Psi_f}, \overline{\Psi_m}) = \int_{I_k} \left(\gamma_f(\overline{\Psi_f} - z)\frac{\partial\Psi_f}{\partial t}, \varphi \right) + J_h^\sigma(\Psi_f, \varphi),$$
$$+ a_{f,h,k}^{L}(\Psi_f, \Psi_m, \varphi, \overline{\Psi_f}, \overline{\Psi_m}) \, \mathrm{d}t \qquad (3.21)$$
$$+ (\gamma_f(\Psi_f - z)|_{k-1}^{+}\Psi_{f,k-1}^{+}, \varphi_{k-1}^{+}),$$

$$A_{m,h,k}^{L}(\Psi_m, \Psi_f, \varphi, \overline{\Psi_f}, \overline{\Psi_m}) = \int_{I_k} \left(\gamma_m(\overline{\Psi_m} - z)\frac{\partial\Psi_m}{\partial t}, \varphi \right) + J_h^\sigma(\Psi_m, \varphi)$$
$$+ a_{m,h,k}^{L}(\Psi_m, \Psi_f, \varphi, \overline{\Psi_f}, \overline{\Psi_m}) \, \mathrm{d}t \qquad (3.22)$$
$$+ (\gamma_m(\Psi_m - z)|_{k-1}^{+}\Psi_{m,k-1}^{+}, \varphi_{k-1}^{+}),$$

and the residual terms as

$$D_{\alpha,h,k}^{L}(\varphi, \overline{\Psi_\alpha}) = \int_{I_k} d_{\alpha,h,k}^{L}(\varphi, \overline{\Psi_\alpha}) + J_D^\sigma(\varphi) \, \mathrm{d}t + (\gamma_\alpha(\overline{\Psi_\alpha} - z)|_{k-1}^{+}\Psi_{\alpha,k-1}^{-}, \varphi_{k-1}^{+})$$

$$(3.23)$$

for $\Psi_f, \Psi_m, \varphi, \overline{\Psi_f}, \overline{\Psi_m} \in S_{h,\tau}^{p,q}$, $\alpha \in \{f, m\}$. Finally, we define

$$\boldsymbol{A}_{h,k}^L(\boldsymbol{\Psi}, \boldsymbol{\varphi}, \overline{\boldsymbol{\Psi}}) = \begin{pmatrix} A_{f,h,k}^L(\Psi_f, \Psi_m, \varphi_f, \overline{\Psi_f}, \overline{\Psi_m}) \\ A_{m,h,k}^L(\Psi_m, \Psi_f, \varphi_m, \overline{\Psi_f}, \overline{\Psi_m}) \end{pmatrix} \tag{3.24}$$

and

$$\boldsymbol{D}_{h,k}^L(\boldsymbol{\varphi}, \overline{\boldsymbol{\Psi}}) = \begin{pmatrix} D_{f,h,k}^L(\overline{\Psi_f}, \varphi_f) \\ D_{m,h,k}^L(\overline{\Psi_m}, \varphi_m), \end{pmatrix} \tag{3.25}$$

where $\boldsymbol{\varphi} = (\varphi_f, \varphi_m)$, $\overline{\boldsymbol{\Psi}} = (\overline{\Psi_f}, \overline{\Psi_m})$.

The forms $A_{\alpha,h,k}^L$ and $D_{\alpha,h,k}^L$ are consistent with the form $A_{\alpha,h,k}$, i.e.,

$$A_{f,h,k}(\Psi_f, \varphi, \Psi_f, \Psi_m) \approx A_{f,h,k}^L(\Psi_f, \Psi_m, \varphi, \Psi_f, \Psi_m) - D_{f,h,k}(\varphi, \Psi_f)$$
$$A_{m,h,k}(\Psi_m, \varphi, \Psi_f, \Psi_m) \approx A_{m,h,k}^L(\Psi_m, \Psi_f, \varphi, \Psi_f, \Psi_m) - D_{m,h,k}(\varphi, \Psi_m) \tag{3.26}$$
$$\Psi_f, \Psi_m, \varphi \in S_{h,\tau}^{p,q}.$$

Let $\boldsymbol{\Psi}$ and $\overline{\boldsymbol{\Psi}}$ be the restrictions to the space $(S_{h,\tau,k}^{p,q})^2$. Using the linearized forms (3.24) and (3.25), we can define the so–called $2N_k \times 2N_k$ flux matrix $\mathbb{C}_{h,k}$:

$$\{\boldsymbol{A}_{h,k}^L(\boldsymbol{\Psi}, \boldsymbol{\varphi}_i, \overline{\boldsymbol{\Psi}})\}_{i=1}^{2N_k} = \left\{ \boldsymbol{A}_{h,k}^L\left(\sum_{j=1}^{N_k} \xi_{f,j} \boldsymbol{\varphi}_j + \sum_{j=N_k+1}^{2N_k} \xi_{m,j} \boldsymbol{\varphi}_j, \boldsymbol{\varphi}_i, \overline{\boldsymbol{\Psi}} \right) \right\}_{i=1}^{2N_k}$$
$$= \left\{ \boldsymbol{A}_{h,k}^L(\boldsymbol{\varphi}_j, \boldsymbol{\varphi}_i, \overline{\boldsymbol{\Psi}}) \right\}_{i,j=1}^{2N_k} \boldsymbol{\xi} =: \mathbb{C}_{h,k}(\overline{\boldsymbol{\xi}}) \boldsymbol{\xi}$$

and the vector $\boldsymbol{q}_h$

$$\mathbf{q}_h(\overline{\boldsymbol{\xi}}) := \{\boldsymbol{D}_{h,k}(\boldsymbol{\varphi}_i, \overline{\boldsymbol{\Psi}})\}_{i=1}^{2N_k},$$

where $\boldsymbol{\varphi}_i$, $i = 1, \ldots, 2N_k$, are the basis functions from (3.18) and $\boldsymbol{\xi}, \overline{\boldsymbol{\xi}} \in \mathbb{R}^{2N_k}$ are the coefficients of $\boldsymbol{\Psi}, \overline{\boldsymbol{\Psi}}$ with respect to the basis $(B_{h,k})^2$, respectively.

Finally, by virtue of (3.26), we obtain the approximation

$$\mathbf{F}_{h,k}(\boldsymbol{\xi}_k) \approx \mathbb{C}_{h,k}(\boldsymbol{\xi}_k) \boldsymbol{\xi}_k - \mathbf{q}_h(\boldsymbol{\xi}_k), \quad k = 1, \ldots, r. \tag{3.27}$$

If we fix the arguments of $\mathbb{C}_{h,k}$ and $\mathbf{q}_h$ perform the differentiation of (3.27) with respect to $\boldsymbol{\xi}_k$, we arrive at

$$\mathbf{J}_{h,k}(\boldsymbol{\xi}_k) \approx \mathbb{C}_{h,k}(\boldsymbol{\xi}_k).$$

Notice that matrix $\mathbb{C}_{h,k}$ and the Jacobian matrix $\mathbf{J}_{h,k}$ are sparse and have block structure. Therefore, we can approximate the Jacobian matrix $\mathbf{J}_{h,k}(\boldsymbol{\xi}_k)$ by the flux matrix $\mathbb{C}_{h,k}(\boldsymbol{\xi}_k)$.

Remark 4. Even though we defined the forms (3.21) and (3.22) using the integration by parts leading to (3.15), it did not cause any of the mentioned problems, since $\mathbb{C}_{h,k}$ is only an approximation of the Jacobi matrix $\mathbf{J}_{h,k}$.

In the end of this section, we will briefly describe a technique for solving (3.19). We will use a Newton-like method described in [11], which is characterized by the fact that the Jacobian $\mathbf{J}_{h,k}$ is replaced by some approximation. We will also employ a damping parameter λ^l, which helps with the convergence, if the initial guess $\boldsymbol{\xi}_k^0$ is far from the solution. This method will generate a sequence $\{\boldsymbol{\xi}_k^l\}_{l=0,1,\ldots}$, approximating an actual numerical solution $\boldsymbol{\xi}_k$. The stopping criterion is discussed in the next section.

Algorithm 1. Damped Newton-like algorithm [2]

1. Let $\boldsymbol{\xi}_k^0 \in \mathbb{R}^{2N_k}$ be given.

2. Until a stopping criterion is not satisfied, compute:

   - Find $\mathbf{d}^l \in \mathbb{R}^{2N_k}$ such that

   $$\mathbb{C}_{h,k}(\boldsymbol{\xi}_k^l)\mathbf{d}^l = -\mathbf{F}_{h,k}(\boldsymbol{\xi}_k^l), \qquad (3.28)$$

   - update

   $$\boldsymbol{\xi}_k^{l+1} = \boldsymbol{\xi}_k^l + \lambda^l \mathbf{d}^l,$$

   where $\lambda^l \in (0,1]$ is a damping parameter such that the monitoring function $\delta^l := ||\mathbf{F}_{h,k}(\boldsymbol{\xi}_k^{l+1})||/||\mathbf{F}_{h,k}(\boldsymbol{\xi}_k^l)||$ is less than 1.

At the start of each step, we set $\lambda^l = 1$ and multiply it by $q = 0.75$ until the monitoring function $\delta^l < 1$. Thus, multiple evaluation of $\mathbf{F}_{h,k}$ can occur in each iteration. The linear system (3.28) is solved by the GMRES method with block ILU(0) preconditioner, see [12] for the details.

3.5   Stopping criteria

It remains to deal with the stopping criterion mentioned in Algorithm 1. We want to avoid stopping the algorithm too early, since the accuracy of the solution can suffer. On the other hand, we do not want stopping criterion too strict, since its computational efficiency can get too low. The solution strategy presented in the previous chapter raises the following sources of errors:

- space discretization,

- time discretization,

- violation of (3.19) by the algebraic solver.

We will use the same technique for balancing these types of errors as presented in [2] and [13].

To introduce error estimators, we will briefly summarise exact, space-time and approximate solutions:

- exact solution $\boldsymbol{\Psi} \in L^2(0,T; H^2(\Omega))^2$ satisfying (2.1),

- space-time discontinuous Galerkin discrete solution $\boldsymbol{\Psi}_{h\tau} \in S_{h,\tau}^{p,q}$ satisfying (3.17) exactly without algebraic errors,

- approximate solution $\overline{\boldsymbol{\Psi}}_{h\tau} \in S_{h,\tau}^{p,q}$ of (3.17) given by the Algorithm 1.

We outline the idea of the error measure in the dual norm. Let V be a linear vector space equipped with a norm $||\cdot||_V$ and V_h a finite dimensional subspace

of V. Let $a(\cdot, \cdot) : V \times V \to \mathbb{R}$ be a form linear with respect to its second argument and $u \in V$, $u_h \in V_h$ be an exact and approximate solution of

$$a(u, \varphi) = 0 \quad \forall \, \varphi \in V, \quad a(u_h, \varphi_h) = 0 \quad \forall \, \varphi_h \in V_h,$$

respectively. Then the error measure in the dual norm on the space V is given by

$$
\begin{aligned}
E(u_h) = ||Au_h - Au||_{V'} &= \sup_{\varphi \in V, \varphi \neq 0} \frac{a(u_h, \varphi) - a(u, \varphi)}{||\varphi||_V} \\
&= \sup_{\varphi \in V, \varphi \neq 0} \frac{a(u_h, \varphi)}{||\varphi||_V},
\end{aligned}
\tag{3.29}
$$

where $\langle Au, \varphi \rangle = a(u, \varphi)$, $u, \varphi \in V$ and $\langle \cdot, \cdot \rangle$ denotes the duality between V and V' [13].

Practically, only $\overline{\boldsymbol{\Psi}}_{h\tau}$ is available, therefore based on (3.29), we introduce an algebraic estimator η_A^k, a space-algebraic estimator η_{SA}^k and a time-algebraic estimator η_{TA}^k

$$
\begin{aligned}
\eta_A^k(\overline{\boldsymbol{\Psi}}_{h\tau}) &= \max_{\boldsymbol{\varphi}_h \in S_{h,\tau,k}^{p,q}, \boldsymbol{\varphi}_h \neq 0} \frac{\boldsymbol{A}_{h,k}(\overline{\boldsymbol{\Psi}}_{h\tau}, \boldsymbol{\varphi}_h)}{||\boldsymbol{\varphi}_h||_X}, \\
\eta_{SA}^k(\overline{\boldsymbol{\Psi}}_{h\tau}) &= \max_{\boldsymbol{\varphi}_h \in S_{h,\tau,k}^{p+1,q}, \boldsymbol{\varphi}_h \neq 0} \frac{\boldsymbol{A}_{h,k}(\overline{\boldsymbol{\Psi}}_{h\tau}, \boldsymbol{\varphi}_h)}{||\boldsymbol{\varphi}_h||_X}, \\
\eta_{TA}^k(\overline{\boldsymbol{\Psi}}_{h\tau}) &= \max_{\boldsymbol{\varphi}_h \in S_{h,\tau,k}^{p,q+1}, \boldsymbol{\varphi}_h \neq 0} \frac{\boldsymbol{A}_{h,k}(\overline{\boldsymbol{\Psi}}_{h\tau}, \boldsymbol{\varphi}_h)}{||\boldsymbol{\varphi}_h||_X}.
\end{aligned}
\tag{3.30}
$$

The space $S_{h,\tau,k}^{p+1,q}$ consists of piecewise polynomial functions over $K \times I_k$ of the degree $\leq p + 1$ with respect to $x \in K$ and the degree $\leq q$ with respect to $t \in I_k$ and vice versa for the space $S_{h,\tau,k}^{p,q+1}$. Obviously, these spaces are bigger than $S_{h,\tau,k}^{p,q}$. The norm $|| \cdot ||_X$ is defined as

$$||\varphi_h||_X = \left(\int_{I_k} \sum_{K \in \mathcal{T}_{h,k}} \left(||\varphi_h||_K^2 + ||\nabla \varphi_h||_K^2 + ||\partial_t \varphi_h||_K^2 \right) \mathrm{d}t \right)^2.$$

The quantity η_A^k measures the violation of (3.17) by an inexactly computed approximation $\overline{\boldsymbol{\Psi}}_{h\tau}$ given by Algorithm 1. The quantity η_{SA}^k (η_{TA}^k respectively) assumes that the approximate solution is formally exact in space (time respectively) and measures the violation of the consistency identity (3.26).

The error estimates defined in (3.30) set the stopping criterion in Algorithm 1 in a following way:

- At each time level, repeat step 2. of Algorithm 1 until

$$\eta_A^k \leq c_A \, \eta_{SA}^k, \quad k = 1, \ldots, r, \tag{3.31}$$

- at each time level, we require

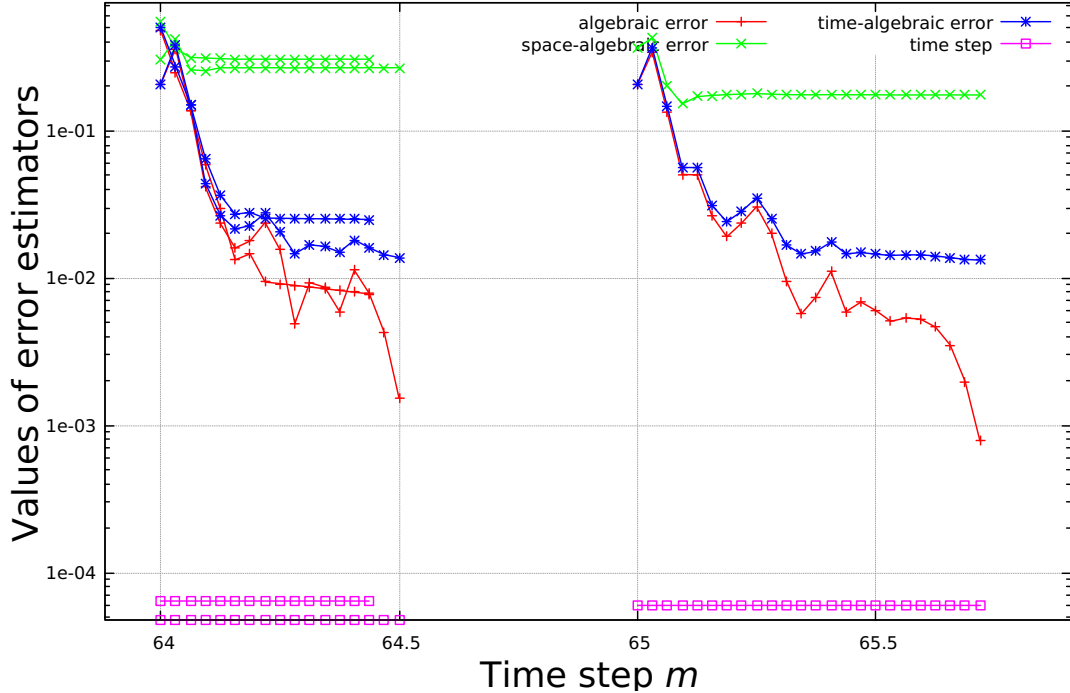$$\eta_{TA}^k \leq c_T \, \eta_{SA}^k, \quad k = 1, \ldots, r. \tag{3.32}$$

Figure 3.1: Example of the convergence of error estimators η_A^k (algebraic), η_{SA}^k (space-algebraic) and η_{TA}^k (time-algebraic) for two time intervals I_k, $k = 64$ and $k = 65$.

We put $c_A = 0.01$ and $c_T = 0.5$ for the experiment in Section 4.1. If the nonlinear algebraic solver in Algorithm 1 does not reach condition (3.31) in prescribed 30 iterations, it will refuse the time step, reduce it by factor 4 and repeat the computation. This is shown in Figure 3.1 on time level 64, where two sets of lines are depicted. If the condition (3.32) is violated, the step is refused and recomputed with smaller time step. In case of the second experiment in 4.2, we put $c_A = 0.1$ with the maximal number of iterations as 60 for each time level and we set $c_T = 0.2$.

Even though this technique is more of a heuristic, the evaluation of the presented estimators is fast and easy to implement.

3.6   Mesh adaptation

In this section, we briefly introduce the idea of anisotropic mesh adaptation, which we are using in our single ring experiment described in Section 4.2. More details about the anisotropic mesh adaptation are in [14], [15] and [13].

This technique is based on the control of the interpolation error of a piecewise polynomial interpolation of the exact solution on the triangular grid [15]. The mesh can be refined locally, which leads to faster computations and smaller memory requirements, unlike the global mesh refinement. Although this method is not based on a posteriori error estimation, which is a commonly used technique for the mesh refinement, it provides high efficiency [14].

Let $\Pi_{h,p,k}$ be an $L^2(\Omega)$ projection onto $S_{h,p,k}$ and let $\omega > 0$ be a given tolerance. The problem is: Find a sequence of meshes $\mathcal{T}_{h,k}$, $k = 1, \ldots, r$ and the polynomial

approximations degrees $p_K \in \mathbb{N}$ such that

- $||\boldsymbol{\Psi}(t_k) - \Pi_{h,p,k}\boldsymbol{\Psi}(t_k)||_{L^\infty(\Omega)} \leq \omega,$

- $\dim(S_{h,p,k})$ is minimal,

where $\boldsymbol{\Psi}$ is the exact solution and $\Pi_{h,p,k}\boldsymbol{\Psi}$ denotes its projection into the space $S_{h,p,k}$. Obviously, the exact solution $\boldsymbol{\Psi}$ is not known, but can be reconstructed from the approximate solution by a higher order reconstruction using the least-square technique, for example as in [16].

Taking into account the stopping criteria from Section 3.5 and the briefly introduced anisotropic mesh adaptation with the Algorithm 1, we can summarize the steps in the following algorithm:

Algorithm 2. Anisotropic space-time discontinuous Galerkin method [2]

1. Let $\omega > 0$, mesh $\mathcal{T}_{h,1}$ and time step τ_1 be given.

2. Put $t = 0$.

3. For $k = 1, \ldots, r$:

   (a) Solve (3.17) using Algorithm 1 for one time step until (3.31) is reached. Let $\overline{\boldsymbol{\Psi}}_{h\tau}$ is the output of Algorithm 1 and set $\overline{\boldsymbol{\Psi}}_{h\tau}^k := \overline{\boldsymbol{\Psi}}_{h\tau}|_{I_k}$.

   (b) If (3.32) is not fulfilled, decrease τ_k and repeat step (a).

   (c) Reconstruct $\overline{\boldsymbol{\Psi}}_k$ from the solution $\overline{\boldsymbol{\Psi}}_{h\tau}^k(t_k^-)$ from Algorithm 1 and verify

   $$||\overline{\boldsymbol{\Psi}}_k(t_k) - \Pi_{h,p,k}\overline{\boldsymbol{\Psi}}_k(t_k)||_{L^\infty(\Omega)} \leq \omega. \tag{3.33}$$

   (d) If (3.33) is violated, create a new mesh $\mathcal{T}_{h,k}$ and the corresponding polynomials degree p_K and repeat step (a).

   (e) Put $t := t + \tau_k$. If $t \geq T$, then stop.

   (f) Set $\mathcal{T}_{h,k+1} := \mathcal{T}_{h,k}$, $\tau_{k+1} = \tau_k$ and go to the next time step.

4. Numerical results

In this chapter, we present several numerical experiments to illustrate the proposed model, whose discretization leads to the system of non-linear equations (3.17) for each time step, which is solved iteratively by the technique from Section 3.4. In first Section 4.1, we verify our model with 1D benchmark problem. Moreover, in Section 4.2, we show and discuss results concerning the single ring experiment, see [17] and [18]. We use the ADGFEM [3] framework for computing all numerical experiments on machine equipped with Intel Q8300 CPU.

4.1 One-dimensional problem verification

We solve the problem (2.1) in a thin rectangular domain Ω, with 40 cm depth and with 0.1 cm width, see Figure 4.1. The mesh consists of 100 elements with finer triangulation close to the surface and the polynomial degrees $p = 3$ and $q = 1$. We use the fixed polynomial degree with respect to the space and the time, respectively. The final time is set as $T = 0.1$ day ($= 144$ min).

(a) Mesh on domain Ω. (b) Detailed mesh at the surface.
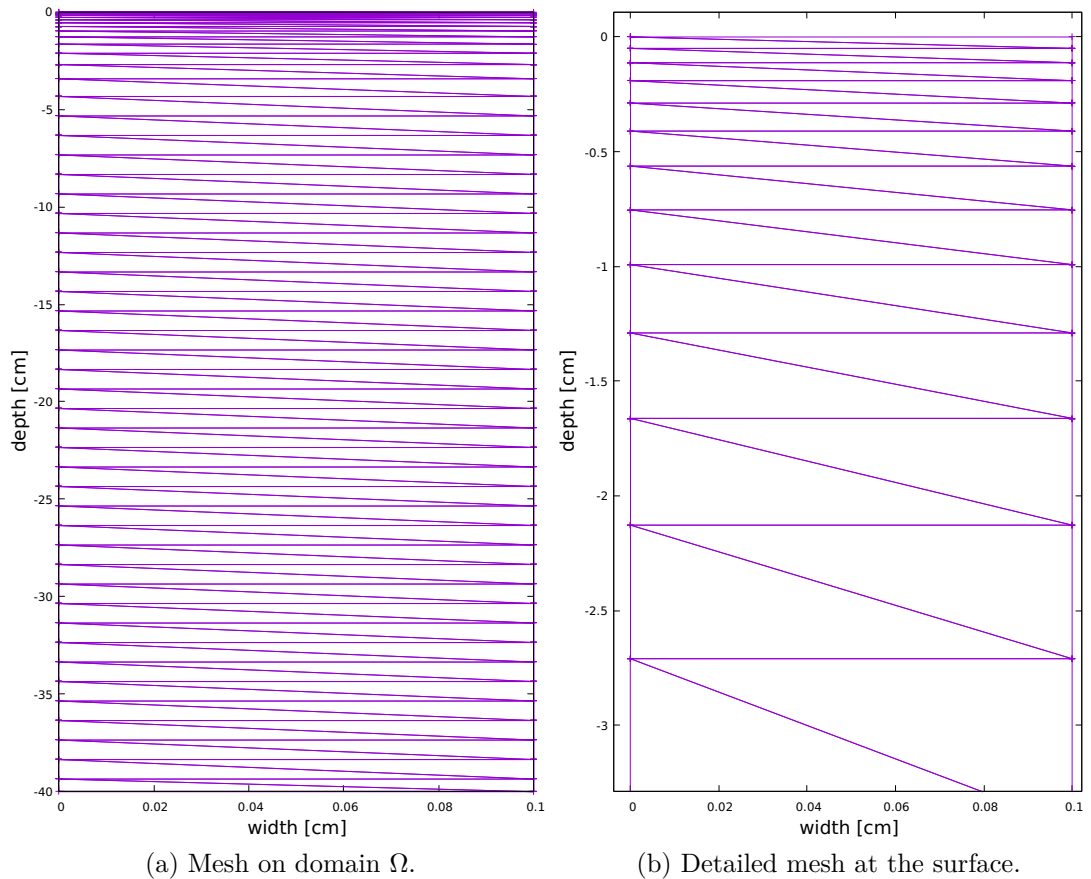
Figure 4.1: Mesh used for 1D verification (different scaling in coordinates).

The parameters describing the hydraulic properties in the van Genuchten function and in the Mualem function are stated in Table 4.2, where $m = 1 - 1/n$.

Further, we prescribe the fracture weight $w_f = 0.05$ and thus the matrix weight is $w_m = 0.95$.

	θ_r	θ_s	α [cm^{-1}]	n	$\mathbf{K}_s$ [cm day^{-1}]	S_s [cm^{-1}]
Fracture $_f$	0.0	0.5	0.1	2.0	2000.0	10^{-7}
Matrix $_m$	0.10526	0.5	0.005	1.5	1.0526	10^{-7}

Table 4.1: Hydraulic parameters used in the experiment.

We prescribe the initial conditions (2.4) as $\Psi_{f_0} = \Psi_{m_0} = -1000$ cm. The boundary conditions are shown in Figure 4.2. The Dirichlet boundary conditions on Γ_1 are given as $\Psi_{D_f} = \Psi_{D_m} = -1000$ cm for the both porous media. We prescribe the Neumann boundary conditions on Γ_2 and Γ_3 as a no flow boundary for the both porous media. However, on Γ_4, we prescribe a flow for the fracture medium, since we allowed the water infiltration only to the fracture medium. We can write the Neumann boundary conditions as follows:

$$\Psi_{N_f} = 0 \quad \text{cm day}^{-1} \quad \text{on } \Gamma_2 \cup \Gamma_3,$$
$$\Psi_{N_m} = 0 \quad \text{cm day}^{-1} \quad \text{on } \Gamma_2 \cup \Gamma_3,$$
$$\Psi_{N_f} = -50 \quad \text{cm day}^{-1} \quad \text{on } \Gamma_4,$$
$$\Psi_{N_m} = 0 \quad \text{cm day}^{-1} \quad \text{on } \Gamma_4.$$
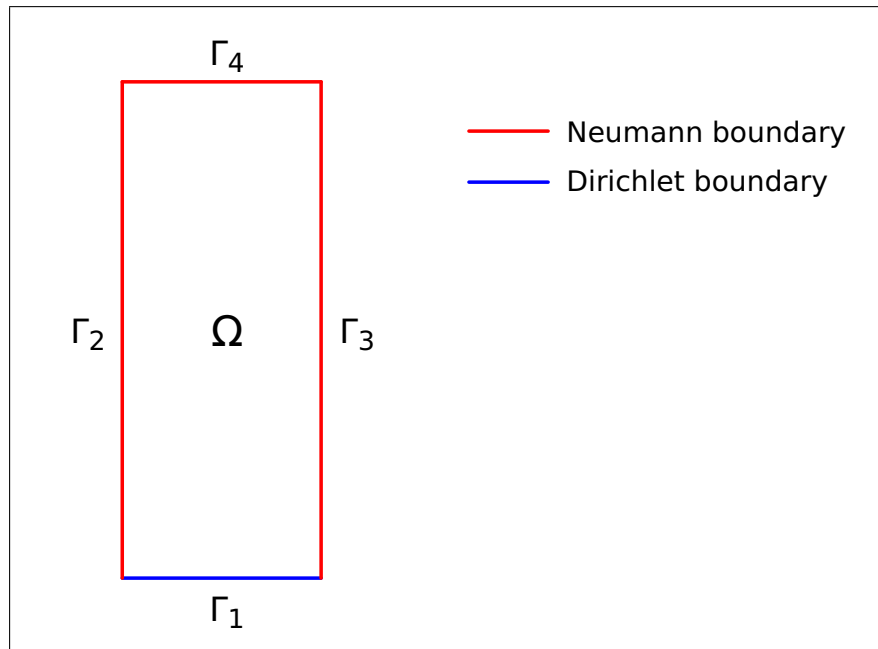
Figure 4.2: Boundary conditions.

Even though the symmetric variant ($\Theta = 1$) of the discontinuous Galerkin method have better theoretical results, we will use the nonsymmetric variant ($\Theta = -1$), because we can set smaller penalty weight and primarily we save computational time, because the resulting linear algebraic systems are easier to solve. We impose the penalty weight $\sigma = 50$.
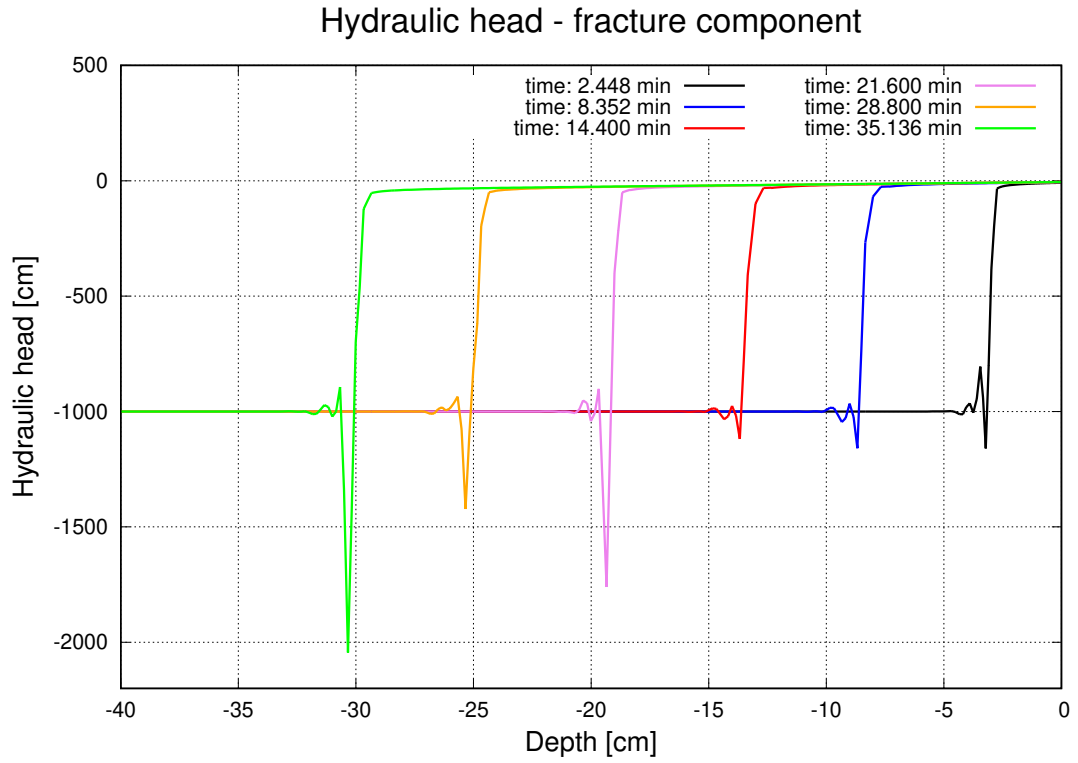
Figure 4.3: Water inflitration with no exchange between the porous media - fracture component ($\Gamma_w = 0$).
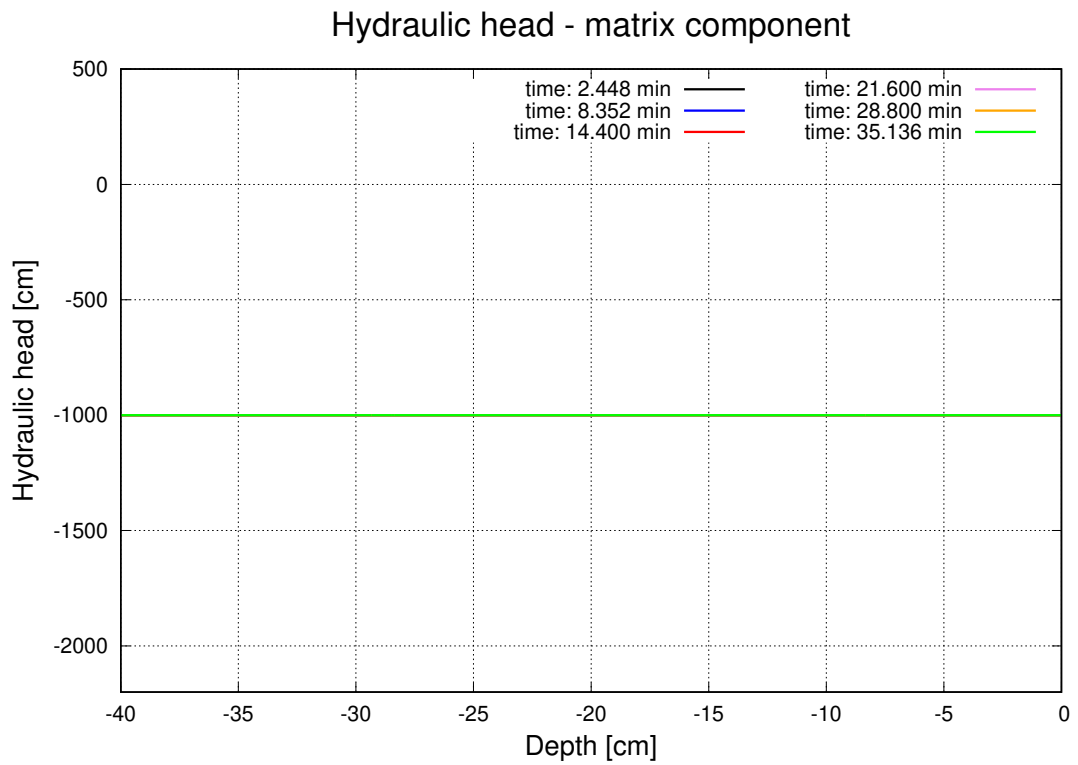
Figure 4.4: Water inflitration with no exchange between the porous media - matrix component ($\Gamma_w = 0$).

The water was allowed to infiltrate only the fracture pore system, thus the water content in the matrix pore system is dependent on the exchange term Γ_w. We remind the form of the exchange term

$$\Gamma_w = \alpha_w(\psi_f - \psi_m), \quad \alpha_w = \frac{\beta}{a^2}\gamma_w K_a.$$

Indeed, if we set $\Gamma_w = 0$ (no exchange of the water between the porous media), we see in Figure 4.4 unchanged hydraulic head for the matrix component. Figure 4.3 shows hydraulic head of the fracture component with no water flow to the matrix porous medium. We observe non-physical oscillations. This is due to steep gradient of the prescribed flow and we also used a relatively coarse mesh because of the computational complexity. However, the oscillations are not growing up (they are "stable"), which is a typical favorable property of the discontinuous Galerkin method. It is possible to reduce them using finer adaptive grids or a stabilization.

We set the parameters as follows: $\beta = 3.0$, $\gamma_w = 0.4$, $a = 1$ cm. Moreover, we redefine the exchange term as

$$\Gamma_w^\delta := \delta\,\Gamma_W,$$

because it is not clear, how it is used in [1]. We experiment with values $\delta = 0.01$ and $\delta = 0.0001$ in order to reduce the influence of the fracture pore system to the matrix pore system.

Figures 4.5 and 4.6 show the progress of hydraulic head on different time levels. In both pictures, the oscillations manifest in the fracture component. Notice that the function corresponding to the matrix component is monotonic. As the water infiltrates through the exchange term, the water flow is progressive and thus there is reason for oscillations. The obtained results are comparable with the results from [1].
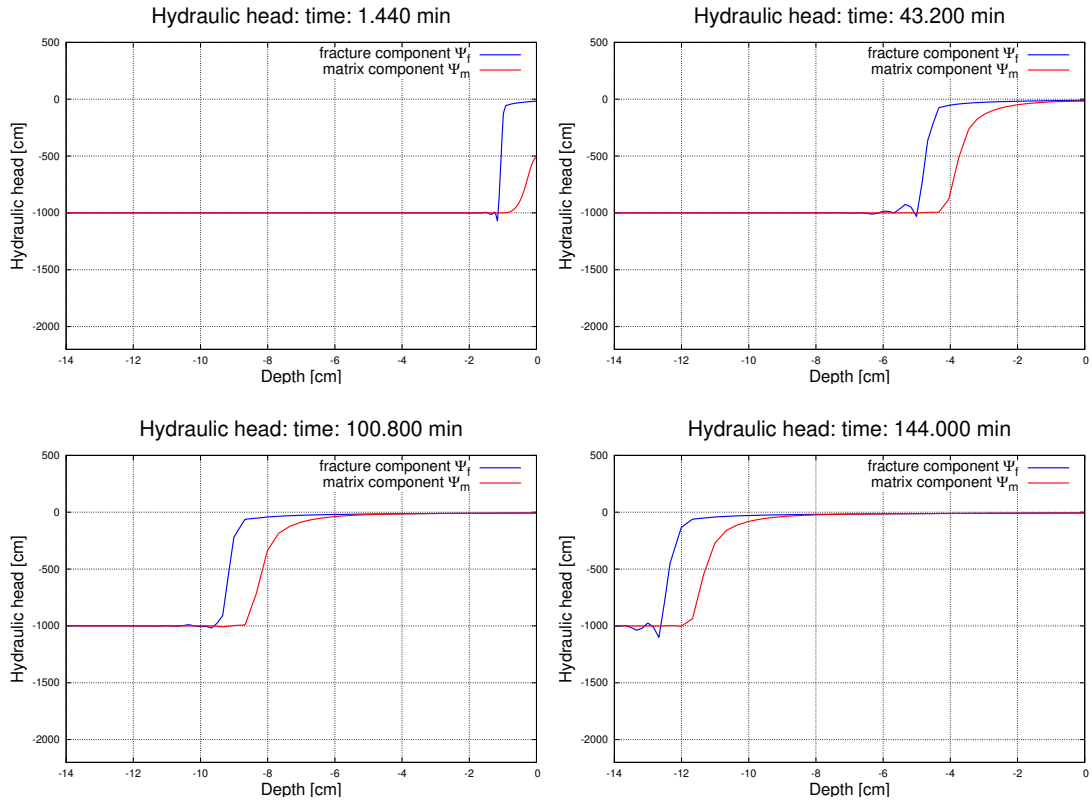
Figure 4.5: Comparison of the hydraulic head with exchange term $\Gamma_w^{0.01}$.
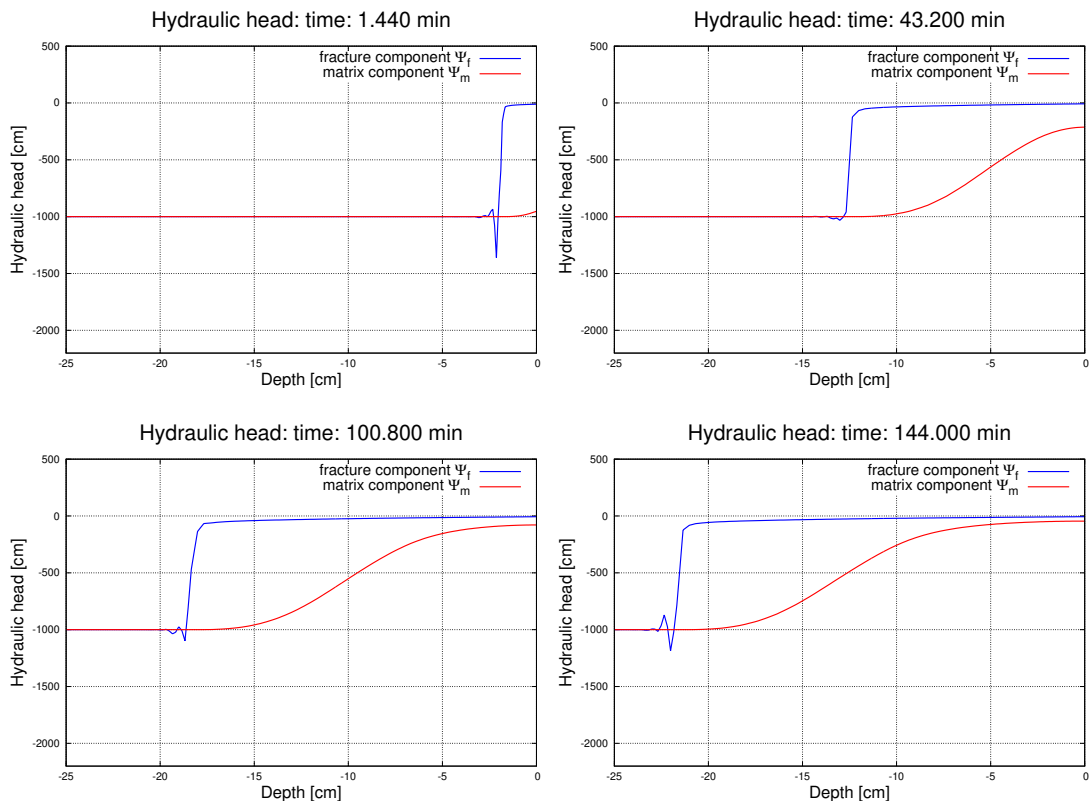
Figure 4.6: Comparison of the hydraulic head with exchange term $\Gamma_w^{0.0001}$.

4.2   Single ring experiment

A single ring experiment is used for the measuring the rate of water which infiltrated into a porous medium. This experiment consists of insertion of the ring into the soil and adding water inside the ring. In our case, the water is supplied at a constant rate, representing the Dirichlet boundary condition, see Figure 4.8.

We solve the problem (2.1) in the rectangular domain Ω. The mesh for the initial time step is depicted in Figure 4.7. We use the varying polynomial degree in space, set as $p = 2$ for the first iteration, and the fixed polynomial degree in time $q = 1$. The final time is set as $T = 2$ s.
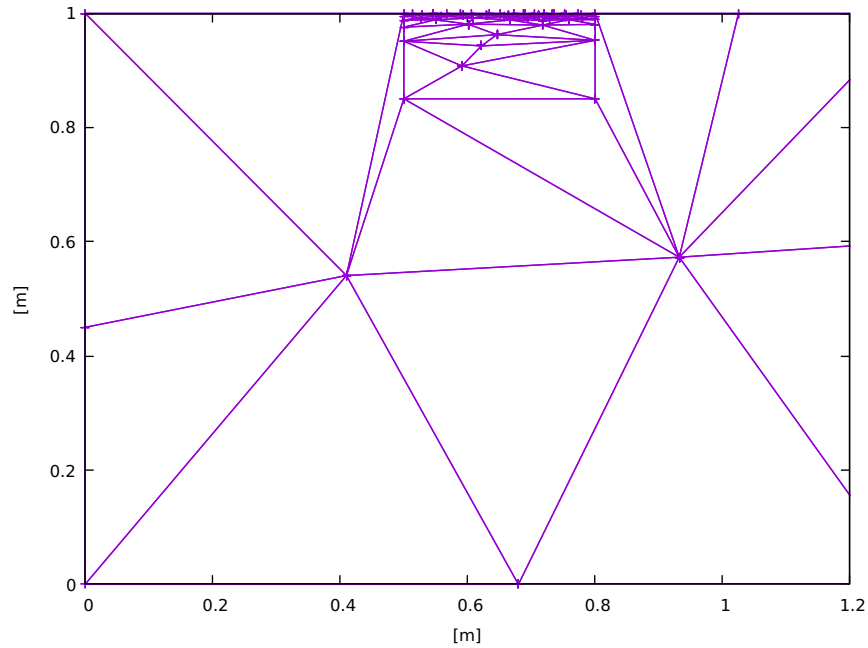
Figure 4.7: Mesh used for single ring experiment.

The parameters describing the hydraulic properties in the van Genuchten function and in the Mualem function are stated in Table 4.2, where $m = 1 - 1/n$. Further, we prescribe the fracture weight $w_f = 0.05$ and thus the matrix weight is $w_m = 0.95$.

	θ_r	θ_s	$\alpha \; [\text{m}^{-1}]$	n	$\mathbf{K}_s \; [\text{m s}^{-1}]$	$S_s \; [\text{m}^{-1}]$
Fracture $_f$	0.0	0.5	0.1	2.0	0.048	10^{-3}
Matrix $_m$	0.10526	0.5	0.005	1.5	0.00002	10^{-3}

Table 4.2: Hydraulic parameters used in the experiment.

We prescribe the initial conditions (2.4) as $\Psi_{f_0} = \Psi_{m_0} = -2$ m. The boundary conditions are shown in Figure 4.8. We prescribe the Dirichlet and the Neumann boundary conditions in the following way:

$$\Psi_{D_f} = 1.05 \quad \text{m s}^{-1} \quad \text{on } \Sigma_D = \Gamma_5,$$
$$\Psi_{D_m} = 1.05 \quad \text{m s}^{-1} \quad \text{on } \Sigma_D = \Gamma_5,$$
$$\Psi_{N_f} = 0 \quad \text{m s}^{-1} \quad \text{on } \Sigma_N,$$
$$\Psi_{N_m} = 0 \quad \text{m s}^{-1} \quad \text{on } \Sigma_N.$$
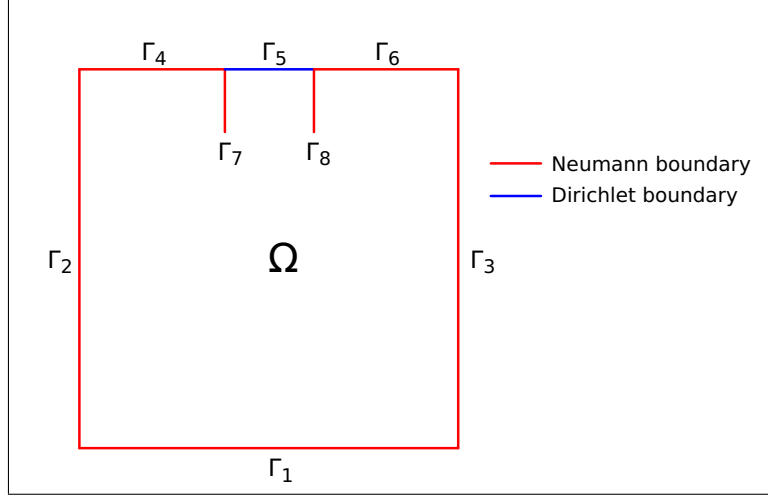
Figure 4.8: Boundary conditions.

We also use the nonsymmetric variant ($\Theta = -1$) for the same reason as mentioned before. We set the penalty weight as $\sigma = 100$.

Figures 4.11 and 4.12 demonstrate the single ring experiment. In this case, we use an adaptive algorithm described in Section 3.6. Figure 4.11 shows the fracture component Ψ_f on the left and the corresponding adapted mesh on the right. Figure 4.12 shows the matrix component on the right instead. We see that the water infiltration is much slower within the matrix component. We also do not see any oscillations that were observed in 4.1.

We introduce a quantity

$$
\begin{aligned}
\boldsymbol{F}(t) = \int_0^t \int_{\Gamma_5} & w_f \left(\mathbf{K}_f(\Psi_f(x,t') - z)\nabla\Psi_f(x,t') \right) \cdot \mathbf{n} \\
& + (1 - w_f) \left(\mathbf{K}_m(\Psi_m(x,t') - z)\nabla\Psi_m(x,t') \right) \cdot \mathbf{n} \, \mathrm{d}S \, \mathrm{d}t',
\end{aligned}
$$

which represents the actual water flux through the boundary Γ_5 accumulated up to the time t. Figure 4.9 shows that the total flux accumulates primarily at the beginning, for both cases – with the adaptation and without the adaptation. Although the results were the same in the first quarter of the simulation, the computational time of the adaptive computation is much smaller than the computation on fixed mesh, see in Figure 4.10. We can observe that in the case of the adaptive algorithm, the time step in the second half of the computation was relatively large and thus the computation finished quickly.

Finally, we also present the development of the mesh adaptation and the comparison of the computational time. Figure 4.13 and 4.14 shows that the mesh was adapted only at the beginning of the simulation. This can be justified by the fact that after the water was fully saturated in the domain delimited by Γ_7 and Γ_8, there were no obstacles, so the time step could be larger. The larger step in the second half of the simulation is also seen in Figure 4.10. Almost all of the computational time was used for the first quarter of the physical time. Figures 4.15 and 4.16 confirm the overall computational time and demonstrate the benefit of the anisotropic mesh adaptation.
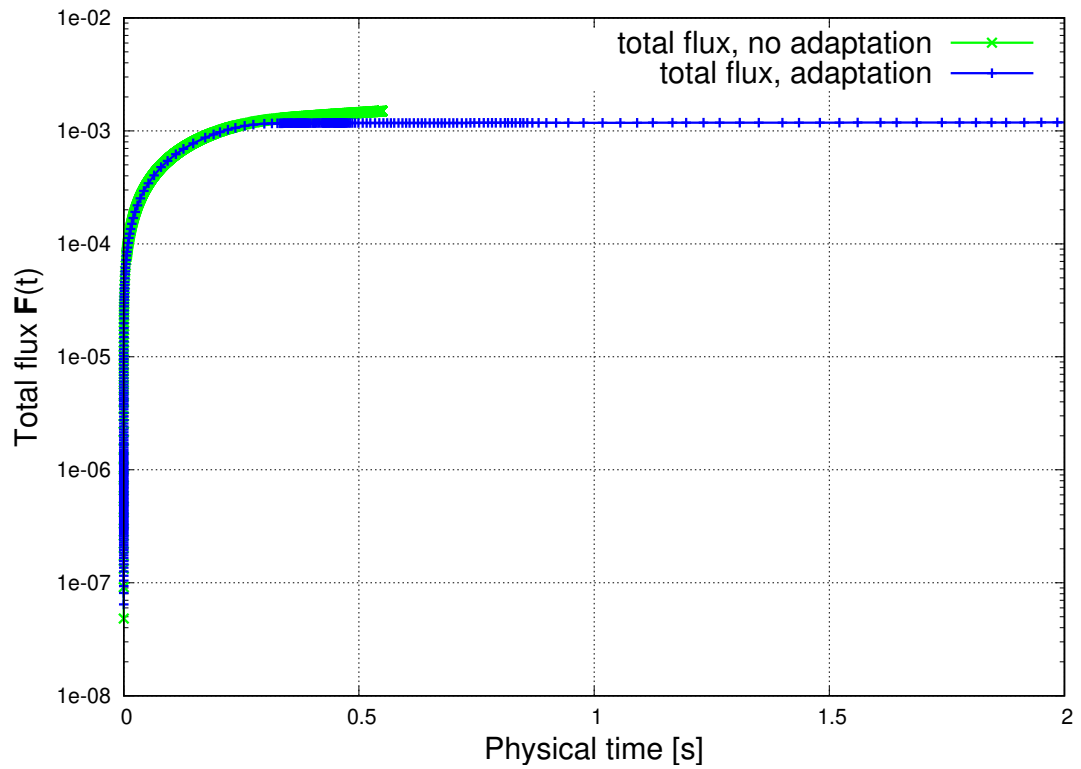
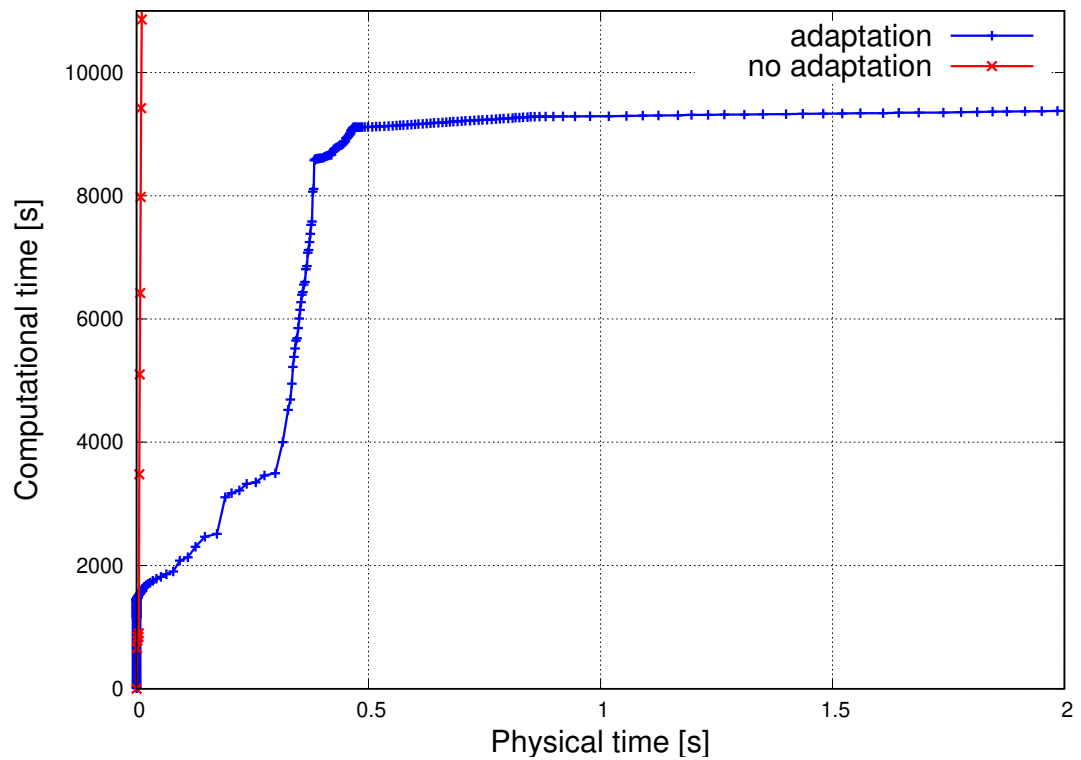Figure 4.9: Accumulated total flux during the simulation.

Figure 4.10: Comparison of computational time of the adaptive algorithm and algorithm without the adaptation.
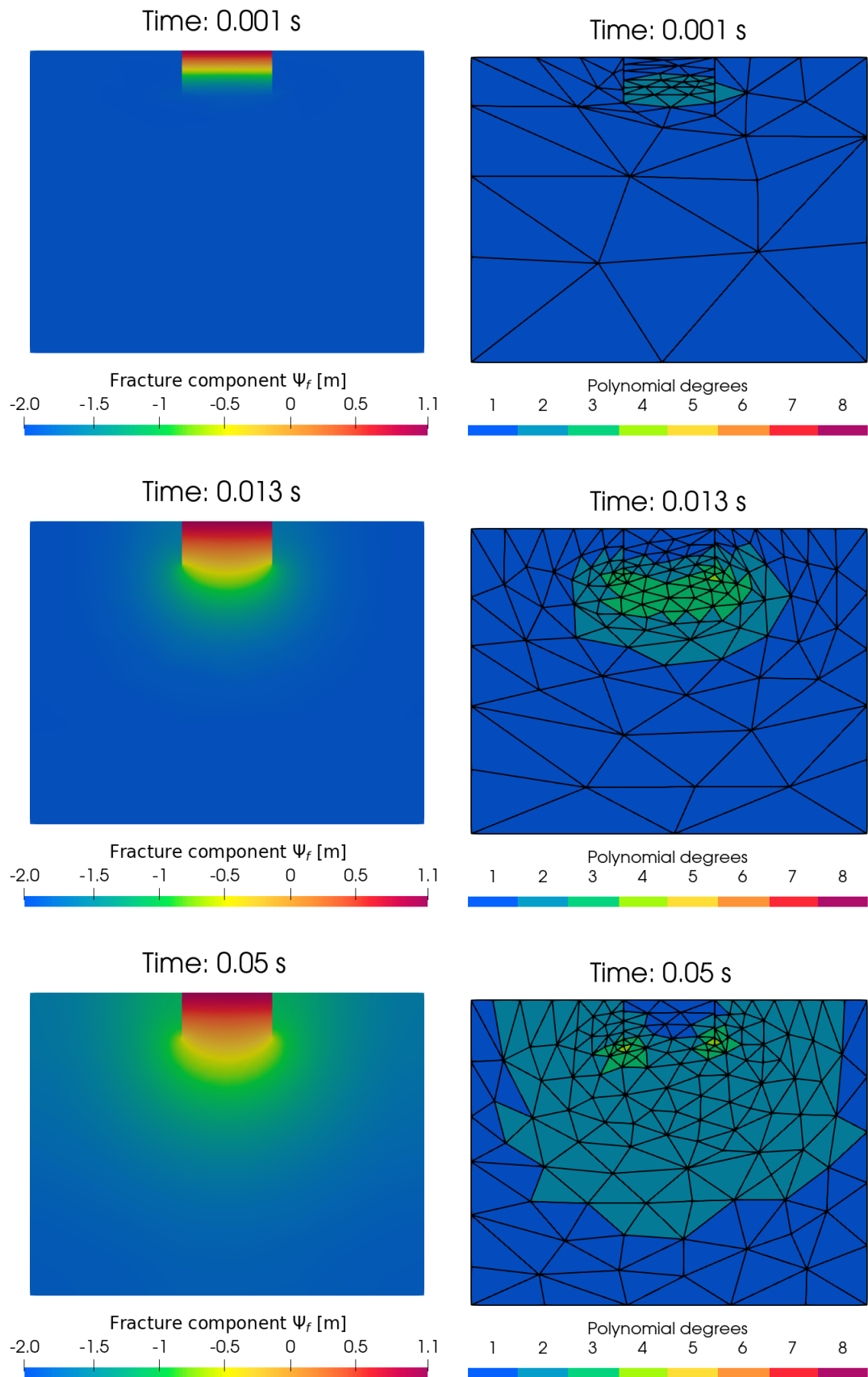
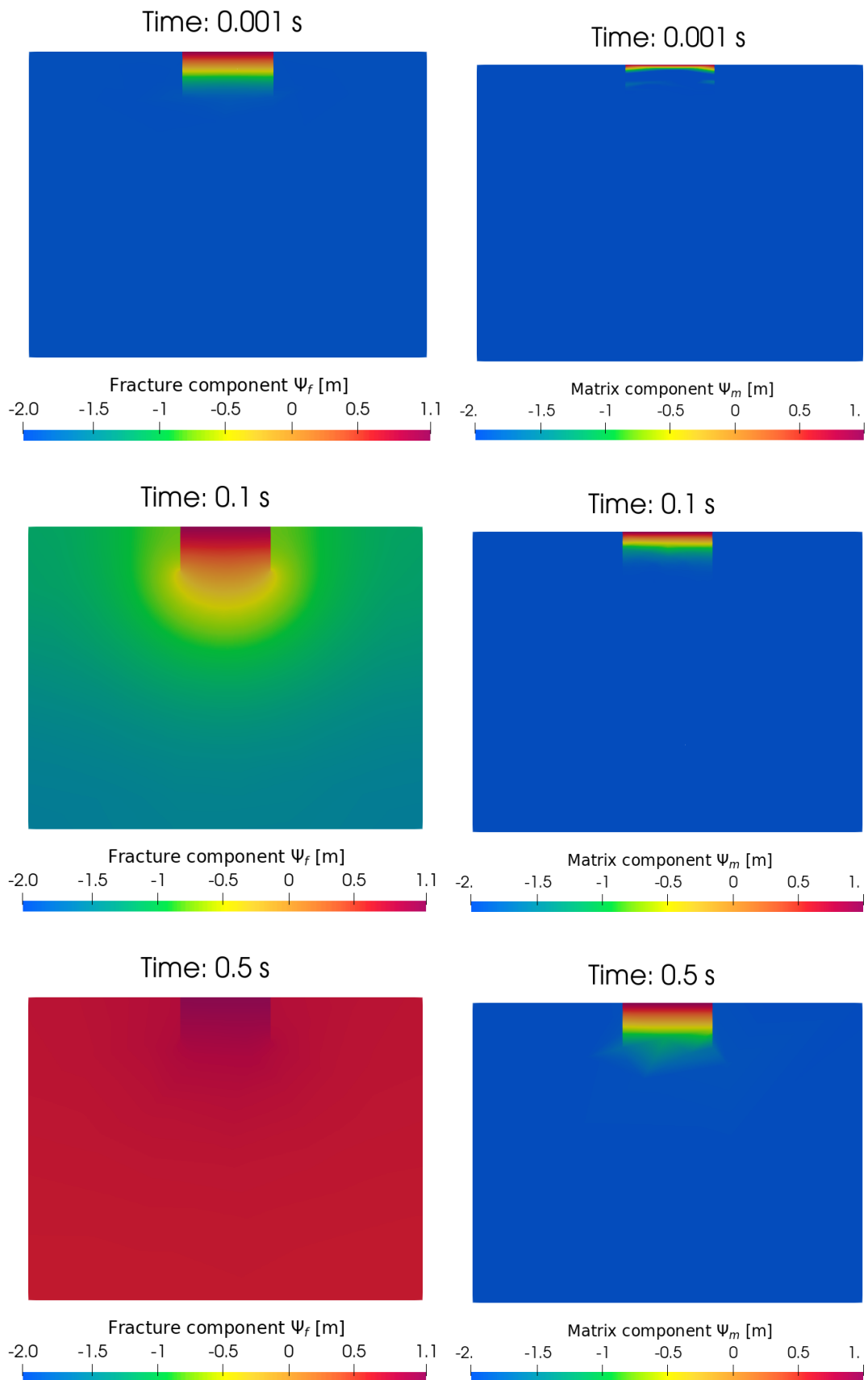Figure 4.11: Hydraulic head – fracture component and adapted mesh.

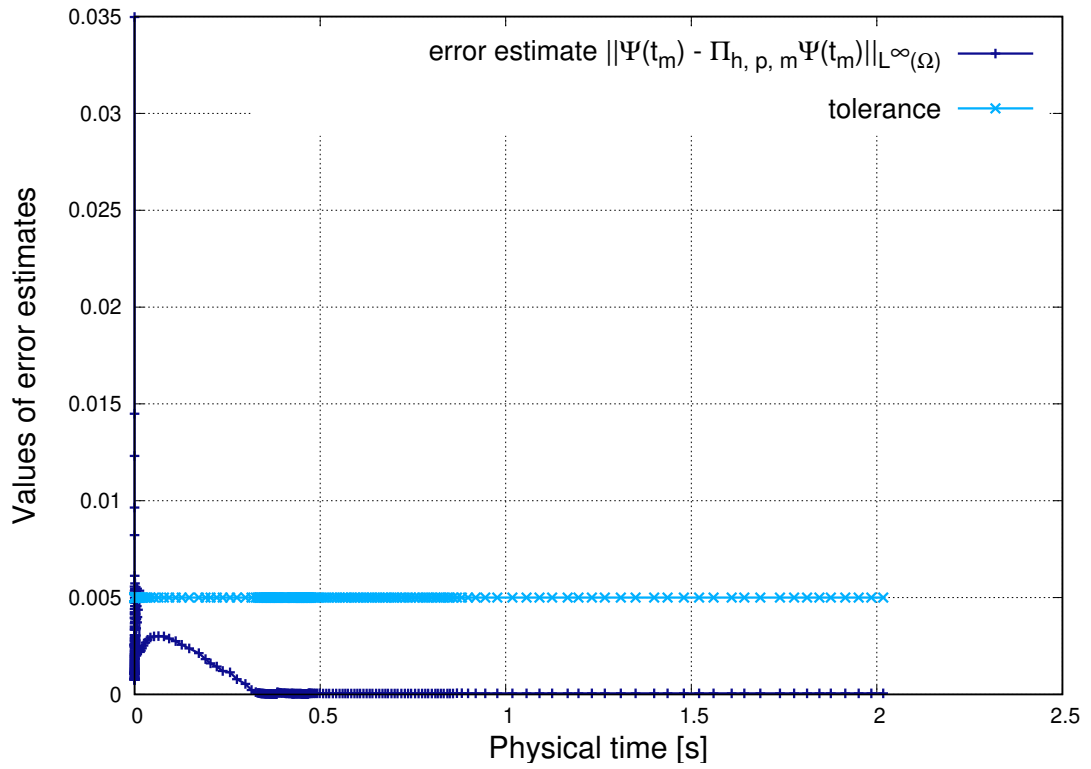Figure 4.12: Hydraulic head – fracture and matrix comparison.

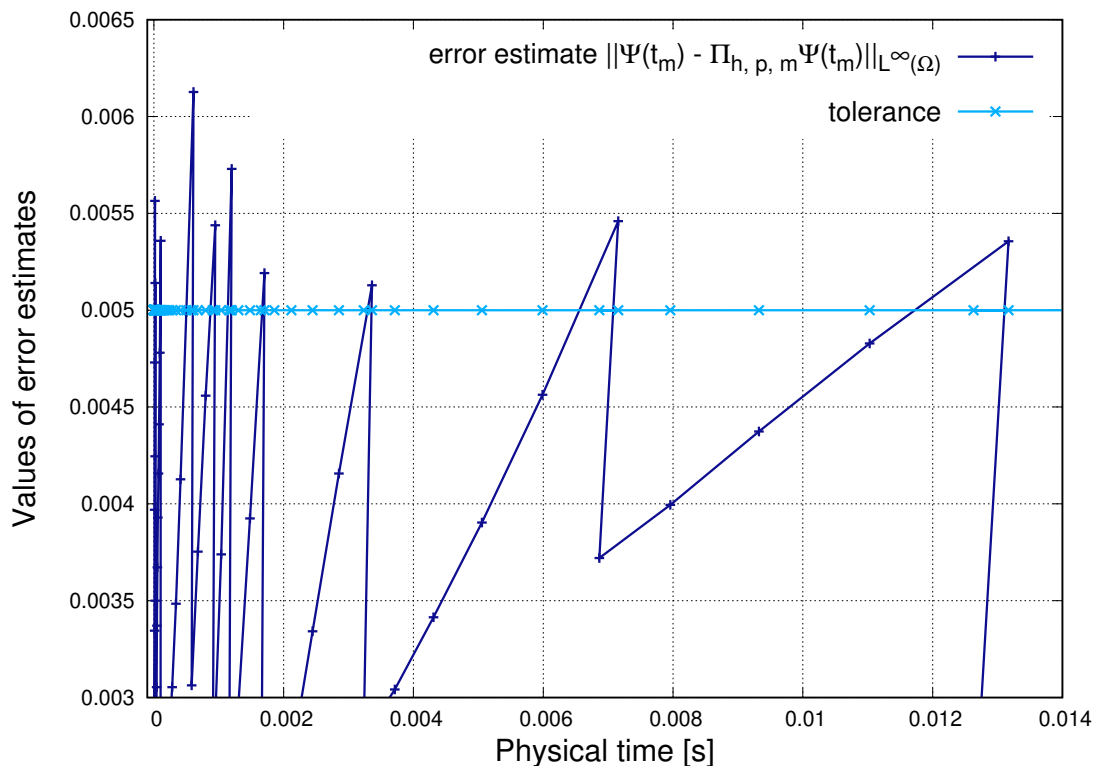Figure 4.13: Representation of the mesh adaptation.

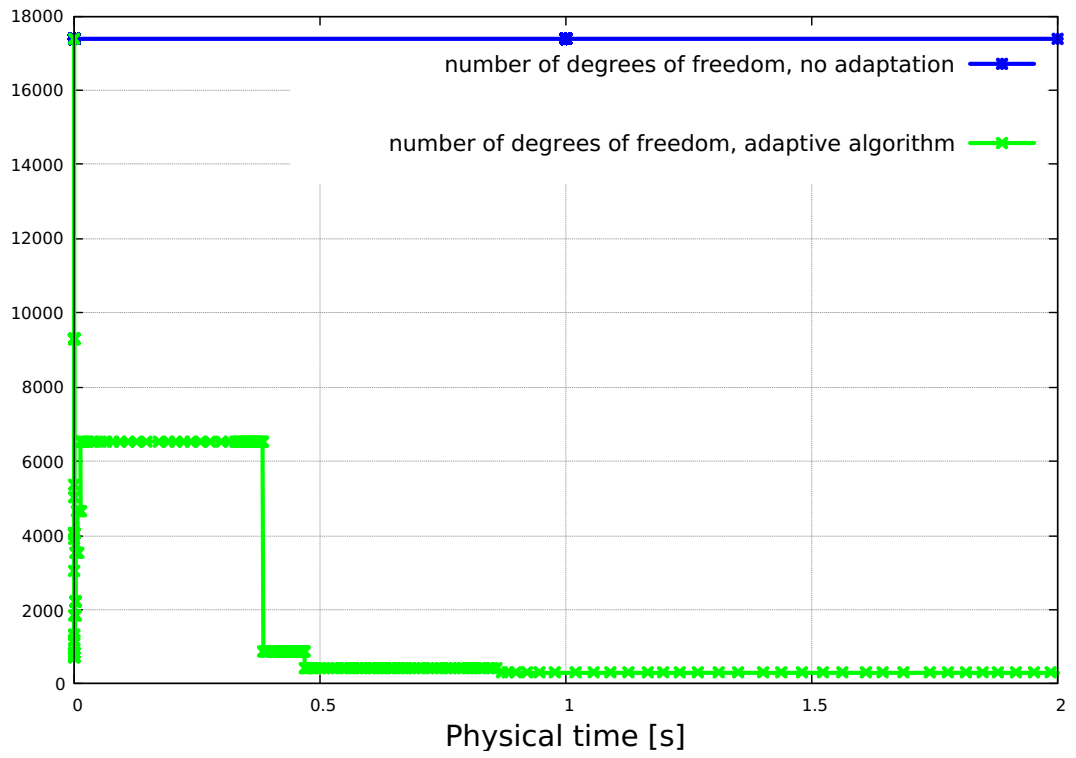Figure 4.14: Representation of the mesh adaptation – detail.
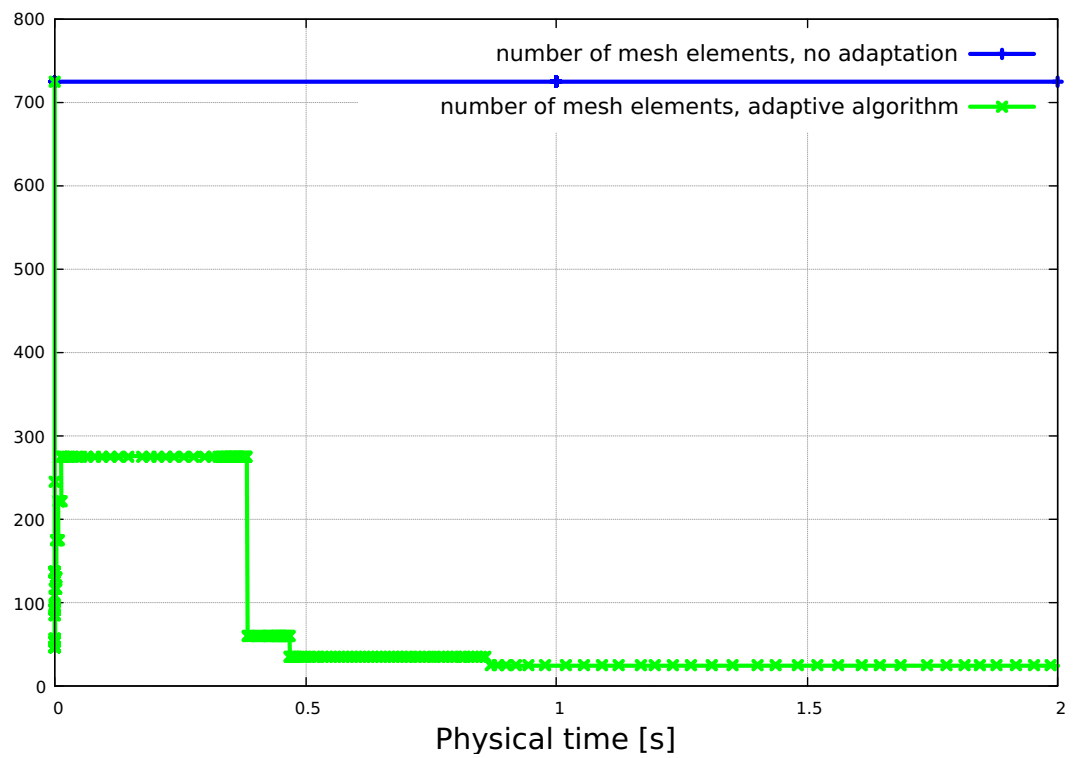
Figure 4.15: Comparison of the number of degrees of freedom.

Figure 4.16: Comparison of the number of mesh elements.

Conclusion

This work deals with the numerical solution of the Richards equation with the dual-permeability model. This concept assumes that the porous media can be separated into two distinct porous media, one with coarse structure (matrix) and the other with finer structure (fracture). We used the space-time discontinuous Galerkin method for the numerical solution.

We derive the Richards equation and afterwards we present the dual-permeability model. The key term in this model is the exchange term, which represents the water exchange between the fracture and the matrix pore systems. The solution of the Richards equation with the dual permeability model is the hydraulic head, which is a vector whose first component represents the fracture pore system and the second component represents the matrix pore system.

The bulk of this work consists of the derivation of the approximate solution using the space-time discontinuous Galerkin method for the dual-permeability model and a technique for obtaining the actual solution. First, we focus on the space discretization and we present the standard tools for the discontinuous Galerkin method. Afterwards, we derive the fully space-time discontinuous Galerkin discretization and we define the discontinuous Galerkin approximate solution of the Richards equation with the dual-permeability model. The solution yields a system of nonlinear algebraic equations. To solve this nonlinear system, we perform linearization and we use a Newton-like method, which consists of replacing the Jacobian of the system by its approximation.

Finally, two numerical experiments are presented. First, we justify our model with a 1D benchmark problem. Even though oscillations manifest in the presented results, the result is still acceptable, since the oscillations are not growing up. The oscillations can be reduced using a finer mesh. The second experiment is the famous single ring infiltration, which is used for the measurement of the rate of water infiltrating into a porous medium. We observe that in the fracture pore system the water infiltration is much faster, which corresponds to the reality. We also experiment with anisotropic mesh adaptation and we compare the overall computational time. The results were the same for the both cases as expected, but with the anisotropic mesh adaption, there is a significant reduction in the computational time.

Bibliography

[1] H. Gerke and M. Van Genuchten. A dual-porosity model for simulating the preferential movement of water and solutes in structured porous media. 29(2):305–319, 1993.

[2] V. Dolejší, M. Kuraz, and P. Solin. Adaptive higher-order space-time discontinuous galerkin method for the computer simulation of variably-saturated porous media flows. *Applied Mathematical Modelling*, 72:276–305, 2019.

[3] V. Dolejší. ADGFEM - adaptive discontinuous galerkin finite element method. `https://www.karlin.mff.cuni.cz/~dolejsi/adgfem/`, Charles University, Prague, Faculty of Mathematics and Physics, 2014.

[4] M. Van Genuchten. A closed-form equation for predicting the hydraulic conductivity of unsaturated soils1. *Soil Science Society of America Journal*, 44:892–898, 09 1980.

[5] M. Kuráž. *Hydrodynamika Porézního Prostředí*. Praha, 2014.

[6] Y. Mualem. A new model for predicting the hydraulic conductivity of unsaturated porous media. *Water Resources Research*, 12:513–522, 1976.

[7] H. Gerke and M. Van Genuchten. Evaluation of a first-order water transfer term for variably saturated dual-porosity flow models. *Water Resources Research*, 29(4):1225–1238, 1993.

[8] F. Otto. L^1–contraction and uniqueness for unstationary saturated-unsaturated porous media flow. *Advances in Mathematical Sciences and Applications*, 7(2):537–553, 1997.

[9] F. Otto. L^1-contraction and uniqueness for quasilinear elliptic-parabolic equations. *Journal of Differential Equations*, 131(1):20–38, 1996.

[10] V. Dolejší and M. Feistauer. *Discontinous Galerkin method*. Praha, 2015.

[11] P. Deuflhard. *Newton Methods for Nonlinear Problems, Springer Series in Computational Mathematics, volume 35*. Springer, 2004.

[12] Y. Saad and M. H. Schultz. Gmres: A generalized minimal residual algorithm for solving nonsymmetric linear systems. *SIAM Journal on Scientific and Statistical Computing*, 7(3):856–869, 1986.

[13] V. Dolejší, F. Roskovec, and M. Vlasák. Residual based error estimates for the space–time discontinuous galerkin method applied to the compressible flows. *Computers Fluids*, 117:304–324, 2015.

[14] V. Dolejší. Anisotropic hp-adaptive method based on interpolation error estimates in the lq-norm. *Applied Numerical Mathematics*, 82:80–114, 2014.

[15] V. Dolejší. *Anisotropic mesh adaptation for finite volume and finite element methods on triangular meshes*. 1998.

[16] V. Dolejší and P. Solin. hp-discontinuous galerkin method based on local higher order reconstruction. *Applied Mathematics and Computation*, 279:219–235, 2016.

[17] V. Dolejší, M. Kuráž, and P. Solin. Numerical simulation of a single ring infiltration experiment with hp-adaptive space-time discontinuous galerkin method. *Acta Polytechnica*, 61:59–67, Feb. 2021.

[18] X. Xu, C. Lewis, W. Liu, J. Albertson, and G. Kiely. Analysis of single-ring infiltrometer data for soil hydraulic properties estimation: Comparison of best and wu methods. *Agricultural Water Management*, 107:34–41, 05 2012.

List of Figures

List of Tables